SOYBEAN OIL BASED RESIN FOR TRANSPARENT FLEXIBLE COATING APPLICATIONS

by

JONGGEUN SUNG

B.S., Kansas State University 2012

A THESIS

submitted in partial fulfillment of the requirements for the degree

MASTER OF SCIENCE

Department of Grain Science and Industry
College of Agriculture

KANSAS STATE UNIVERSITY
Manhattan, Kansas

2014

Approved by:

Major Professor
Xiuzhi Susan Sun

Copyright

Abstract

Soybean oil-based resin for transparent flexible coating applications were formulated by dihydroxyl soybean oil (DSO) with commercial epoxy monomers (i.e., epoxidized soybean oil (ESO) and 3,4-epoxycyclohexylmethyl-3,4-epoxycyclohexanecarboxylate (ECHM)). The resin was formed to thermoset polymers using cationic ring-opening photopolymerization. The ether crosslinking and post-polymerization of the polymeric network were observed using Fourier transform infrared spectroscopy. Thermal properties of the bio-based coating materials and their copolymerization behaviors were examined using a differential scanning calorimetry and a thermogravimetric analyzer. Crosslink density and molecular weight between crosslink were obtained from dynamic mechanical analysis. ECHM/DSO (1: 1.43 weight ratio) films showed the highest elongation at break (49.2 %) with a tensile strength of 13.7 MPa. After 2 months storage, the elongation at break and tensile strength of films were 32 % and 15.1 MPa, respectively. ESO/DSO films (w/w ratios of 1:0.1, 1:0.15, and 1:0.2) exhibited stable flexibility around 11-13 % of elongations at break without significant reductions of tensile strengths (2.5 to 4.4 MPa) during 2-months shelf life. Optical transparencies of the films were comparable to commercial glass and polymers, and water uptake properties (0.72 and 2.83%) were significantly low.

Table of Contents

List of Figures

List of Tables

Acknowledgements

I would like to appreciate to my major professor, Dr. Xiuzhi Sun, for financial support and guiding me to study this master thesis. Also, thanks to my committee members, Dr. Donghai Wang and Dr. Ping Li, for helpful comments.

Thanks to graduate coordinator, Beverly McGee, and Administrative Specialist, Susan Kelly, for helping me all the time. Also, I express my appreciation to Dr. Yonghui Li for answering my questions and supporting lab works, and thanks to all lab members of Bio-materials and Technology Lab and all staff of Grain Science and Industry.

Finally, thanks to my wife, Jiyee Yoon, and my family for supporting and encouraging me always.

Chapter 1 - Introduction

The most widely used coating materials for packaging applications are polyethylene, polyethylene terephthalate, polyvinyl alcohol, and fluorocarbon which are synthesized from petroleum resources. Even though the synthetic polymers show excellent performance properties and competitive price, a demand for bio-plastics has been rapidly increased because most of the petrochemical materials are not biodegradable (Chan and Krochta, 2001; Khwaldia et al., 2010). In addition, environmental regulations have consolidated to protect the earth from chemical pollutants and save the fossil fuel reservoir. Academia and industry have been seeking sustainable alternatives to the petroleum-based materials (Crivello and Narayan, 1992; Meier et al., 2007). Several bio-based polymers such as proteins and polysaccharides have been researched as raw materials for packaging applications (Khwaldia et al., 2010), but their hydrophilic natures lead to poor water resistance (Avenabustillos and Krochta, 1993; Kester and Fennema, 1986). On the contrary, plant oils can be incorporated in the coating materials without loss of water barrier properties (Khwaldia et al., 2010). Moreover, plant oils also possess the advantages of intrinsic biodegradability and low toxicity (Xia and Larock, 2010). Now days, plant oils become one of the most important resources for renewable materials in chemical industries such as surfactants, lubricants, paints, resins, adhesives, and coatings (Meier et al., 2007; Xia and Larock, 2010). Epoxidation of plant oil is commonly used to produce functionalized olefin due to its economical process and significantly improved reactivity of the oils (Holland et al., 2003a; Williams and Hillmyer, 2008).

Photopolymerization has the advantages of fast curing and low energy consumption. Photoinitiated cationic polymerization is commonly used in polymers industries for coatings, adhesives, and printing inks (Crivello and Liu, 2000; Golaz et al., 2012). It is also one of

common curing methods for epoxy resins such as epoxidized soybean oil (ESO) and 3,4-epoxycyclohexylmethyl-3,4-epoxycyclohexanecarboxylate (ECHM) (Ahn, Sung, Kim et al., 2013; Crivello and Narayan, 1992; Decker et al., 2001; Shibata et al., 2009; Voytekunas et al., 2008). Photopolymerized cycloaliphatic resins such as ECHM showed excellent rigidity and adhesion to substrate, and high glass transition temperature (Golaz et al., 2012; Voytekunas et al., 2008), but the brittleness of the epoxy polymer has been a problem for flexible packaging coatings (Luetzen et al., 2013). Previous work in our lab has identified that UV copolymerization of ESO, rosin ester, and soy polyols (i.e., dihydroxyl soy bean oil (DSO)) has interesting flexibility, thermal stability, and optical transmittance, which has potential for flexible coatings (Ahn et al., 2013). In addition the soy polyols improved the softness and tackiness of ESO-based resin (Ahn et al., 2011a; Ahn et al., 2011b). In this study, ESO and ECHM were used as examples of bio-based and non-bio-based epoxy resins, respectively. DSO was formulated into the epoxy resins to improve flexibilities of the epoxy-based polymers. Both ESO/DSO and ECHM/DSO resins were photopolymerized to form copolymers for coating applications.

Objectives

The purpose of this study was to investigate copolymeric bio-based coating materials of DSO with commercial epoxy monomers such as ESO and ECHM to determine that the soybean-based polyol improve flexibilities of the epoxy polymers without reductions of thermal stability and optical transparency.

The objectives of this study were to:

1. Develop resins for bio-based coating materials through optimization of formulations of bio-based resin with petrochemical copolymer
2. Characterize properties of the resin films for mechanical, dynamic mechanical, thermal, and optical transparency properties.

3. Examine post-polymerization effect and shelf-lives of the newly developed bio-based coating materials.

Chapter 2 - Literature Review

Fatty acids

Oleochemicals are attained from renewable resources which are plants oils and animal fats. Natural fats and oils are significant sources as raw materials in oleochemical industry due to its good biodegradability and no greenhouse gas emission (Mol, 2002). Plant oils are mainly composed of triglycerides; triesters of glycerin and three fatty acids which are commonly unsaturated (i.e., oleic, linoleic, and linolenic) and saturated (i.e., palmitic and stearic) (Williams and Hillmyer, 2008). Saturated fatty acids chains are fully filled with hydrogen. On the contrary, unsaturated fatty acids have one or more carbon-carbon double bonds on their aliphatic long chains (Guner et al., 2006). Fatty acid compositions of various plant oils are described (Table 2.1) (Z. Petrovic, 2008). In material science point of view, the olefin of triglycerides monomers is attractive because it could be cross-linked to polymers directly (Kundu and Larock, 2005). Although unsaturated fatty acids have olefins as active sites, the carbon double bonds could not be easily used to directly convert polymer without better reactive functional groups such as epoxy and hydroxyl group (Del Rio et al., 2010). Double bonds of triglycerides can be used to be polymerized, and the active sites can be synthesized through using same methods in petrochemical-based polymers productions (Wool and Sun, 2005). Wool and Sun illustrated several synthetic pathways to functionalized triglycerides and monoglycerides from a natural triglyceride, and the modified triglycerides and monoglycerides are polymerized through using ring-opening, polycondensation, or free-radical polymerization (Figure 2.1). Briefly, the natural triglyceride (Figure 2.1-1) can be modified at unsaturated sites, glycerol sites, or both unsaturated and glycerol sites. Firstly, the unsaturated carbons of the triglyceride are possible to attach maleates (Figure 2.1-5), or it can be converted to epoxy (Figure 2.1-7) or hydroxyl groups

(Figure 2.1-8). The maleates or epoxy modified triglycerides can be polymerized by ring-opening methods, and the hydroxylated triglyceride is possible to be polymerized by polycondensation method. Moreover, the acrylates modified triglyceride (Figure 2.1-6) from the epoxy functional triglyceride can be polymerized by free-radical polymerization. In addition, the hydroxylated triglyceride is converted to maleate half-esters and esters triglycerides (Figure 2.1-11) which is possible to free-radical polymerization. Secondly, the glycerol site of the natural triglyceride is converted to monoglycerides through glycerolysis reaction (Figure 2.1-3A,-3B) or amidation reaction (Figure 2.1-2). The monoglycerides can be polymerized by polycondensation method. Then, maleinized monoglyceride with unsaturated fatty acid (Figure 2.1-9), which are derived by reaction of hydroxyl groups at monoglycerides with maleic anhydride, can be polymerized through using free-radical polymerization. In addition, hydroxylated monoglyceride (Figure 2.1-4) is converted from the monoglyceride (Figure 2.1-3A,-3B) based on hydroxylation at unsaturated carbons of the monoglyceride. Then, the hydroxylated monoglyceride is reacted with maleic anhydride to form saturated maleinized monoglyceride (Figure 2.1-10), which is also possible to free-radical polymerization.

Table 2.1: Typical fatty acid compositions (%) of selected plant oils (Z. Petrovic, 2008)

Carbon atoms:															
Double bonds	8:0	10:0	12:0	14:0	16:0	16:1	18:0	18:1	18:2	18:3	20:0	20:1	22:0	22:1	24:0
Canola				0.1	4.0	0.3	1.8	60.9	21.0	8.8	0.7	1.0	0.3	0.7	0.2
Coconut	7.1	6.0	47.1	18.5	9.1		2.8	6.8	1.9	0.1	0.1				
Corn				0.1	10.9	0.2	2.0	25.4	59.6	1.2	0.4		0.1		
Linseed					6.0		4.0	22.0	16.0	52.0	0.5				
Olive					9	0.6	2.7	80.3	6.3	0.7	0.4				
Palm			0.1	1	44.4	0.2	4.1	39.3	10	0.4	0.3		0.1		
Rapeseed				0.1	3.8	0.3	1.2	18.5	14.5	11.0	0.7	6.6	0.5	41.1	1.0
Soybean				0.1	10.6	0.1	4.0	23.3	53.7	7.6	0.3		0.3		
Sunflower				0.1	7.0	0.1	4.5	18.7	67.5	0.8	0.4	0.1	0.7		

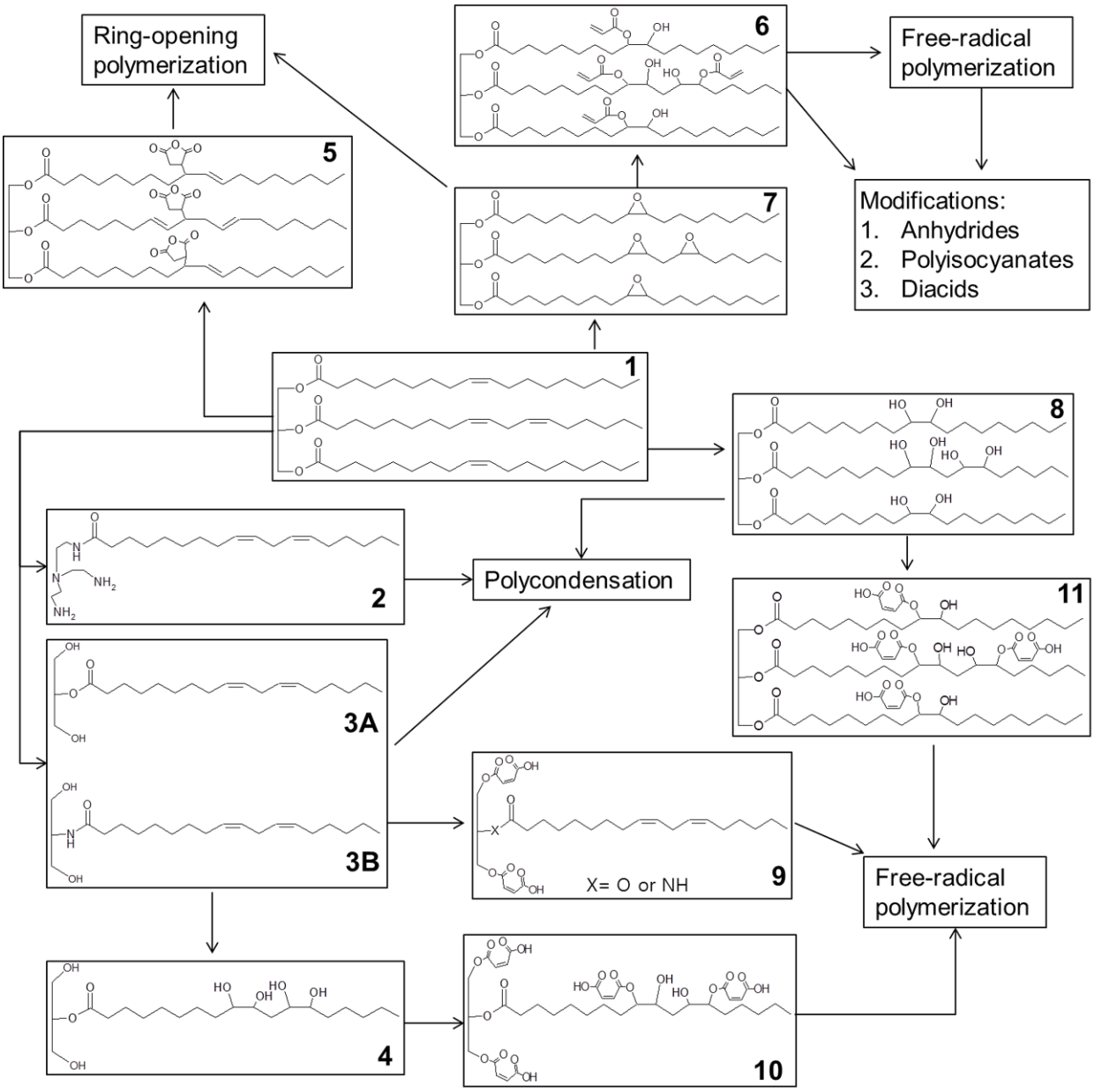

Figure 2.1: Synthetic pathways to modified triglycerides and monoglycerides from a natural triglyceride (Wool and Sun, 2005).

Soybean oil is the most applicable raw material among plants oils in North America because of the large composition of unsaturated fatty acids with low price. (Z. Petrovic, 2008). Soybean oil is composed with 20-25 % of saturated and 80-85 % of unsaturated fatty acids (Mihail and Petrovic, 2011). Mainly, the saturated fatty acids are palmitic (C16:0) and stearic

(C18:0), and the unsaturated fatty acids are oleic (C18:1), linoleic (C18:2), and linolenic (C18:3). Linoleic is a major fatty acid that comprises 50-55 % of a soybean oil triglyceride, and oleic acid is a second largest composition (23-25 %) of a soybean oil. Mihail and Petrovic defined that average molecular weight of soybean oil is 874 g/mol, and 4.6 carbon-carbon double bonds are estimated in a mole of soybean oil.

Epoxidation of plant oil is economical and high efficient since its conversion rates are more than 98% (Holland et al., 2003b), and it is one of the majority plants oil usages in industries with 200,000 tons of annual production (Gunstone, 2004). Epoxidized soybean oil (ESO) has been used to improve flexibility and stability of commercial polymer such as polyvinyl chloride (PVC) and polyvinyl alcohol (PVA) (Guner et al., 2006; Z. Liu et al., 2005; Z. Petrovic, 2008). Currently, ESO is a well-known renewable resource which is commercially applicable to polymer products such as adhesives, coatings, plasticizers, lubricants, and composites. (Chen et al., 2010).

Functionalized ESO monomers

ESO has been widely functionalized to be used at various polymerizations. Rigid and glassy thermoset materials were derived from modified ESO (Luo et al., 2011). From the research, allylic double bonds were added to oxirane rings of ESO by oxirane ring-opening reaction. Then, the allylated ESO was copolymerized with maleic anhydride to form thermosets using free radical polymerization and esterification. Storage modulus, glass transition temperatures, tensile modulus, and tensile strength were enhanced as maleic anhydride content was increased in the thermoset. However, the flexibility was down to the lowest elongation (7 %) containing 30 wt % of maleic anhydride while highest Young's modulus, tensile strength, and glass transition temperature were obtained up to 1 GPa, 29 MPa, and 123 °C, respectively.

Bio-based epoxy resins were obtained to prepare thermoset using maleic anhydride (MA) treated ESO (Espana et al., 2012). Epoxides of ESO were initially modified by maleic anhydride with 1,3-butanediol anhydrous as catalyst, and the treated ESO were thermally cured at a temperature range of 100-160 °C. The synthesized ESO thermoset showed the highest curing degree and optimum properties balances of bending, hardness and impact test when ESO and MA were reacted at equivalent weight ratio of 1:1 (54.8 g of ESO: 22.6 g of MA). Similarly, maleinized polybutadiene were grafted on ESO to synthesize bio-based thermoset polymers (Ozturk and Kusefoglu, 2011). In order to increase the crosslink density of the thermoset matrix, benzoyl peroxide was added as a free-radical initiator. The highest yield of the polymers (91.5%) was found while the molar ratio of epoxy to maleic anhydride was 1:1, and also the highest modulus was obtained at 1:1 of the molar ratio.

Thiol-ene reaction was used to functionalize ESO to synthesize soy-based thiols and enes, which were formulated with petrochemical-based thiols and enes through using free-radical polymerization to produce UV-curable coatings (Chen et al., 2010). The soy-based thiols and enes coating did not show impressive coating properties such as tensile modulus, elongation, thermal degradation, and glass transition temperature. However, the research showed that the coating properties could be improved by addition of acrylates.

Acrylic oligomers and monomers are key components of free-radical photopolymerization, and they are important raw materials in UV-curable coating industries such as coating, adhesives, and composites (Inan et al., 2001; Rengasamy and Mannari, 2013). However, petrochemical-based acrylate derivatives are definitely non-biodegradable and not carbon neutral products. In addition, acrylate derivatives and their diluents such as styrene showed several limitations such as skin irritancy, poor pigment wetting, and film shrinkage

although the petrochemical-based raw materials promise excellent performances for commercial goods (Rengasamy and Mannari, 2013). Acrylated epoxidized soybean oil (AESO) and soybean oil derivative diluent, which is acrylated fatty acid methyl ester-based monomer, were studied to minimize these limitations of petrochemical-based acrylates and their diluents (Campanella et al., 2009). Transparent pressure sensitive adhesives (PSA) were derived from AESO through using photoinitiated free-radical polymerization without any additives such as photoinitiator, diluents, or tackifier, and the PSA showed excellent tack properties on human skins and shear strength in compared with commercial reusable PSA such as Post-it (Ahn, Sung, Rahmani et al., 2013). AESO is commonly obtained from reaction of epoxidized soybean oil with acrylic acid or methacrylic. Currently, flame resistance coating materials were synthesized from a new AESO, which was derived from ESO with methacrylic acid and vinyl phosphonic acid as a flame retardant additive (Basturk et al., 2013). AESO has been used in UV-curable coatings and adhesives industries, but the generally high viscosity of AESO needs reactive diluents to reduce viscosity (Wu et al., 2011). Low viscous acrylated soybean oil derivatives were derived from ESO and epoxidized soy-methyl ester through using 2-hydroxyethyl acrylate with acid catalyzed esterification (Rengasamy and Mannari, 2013). From the research, acrylated epoxidized soy-methyl ester (AEME) exhibited extremely low viscosity (109 cPs at 25 °C) in compared with viscosity of commercial polyester acrylate (70,000 cPs at °25C) while the synthesized AESO had a viscosity (5406 cPs at °25C).

Polyol applications

Because of all-purpose applications, polyurethanes have been attractive polymers since they were invented in the 1940s (Seydibeyoglu et al., 2013). Simply, polyurethane is synthesized with polyol and isocyanate. In order to satisfy desired properties of versatile purposes of

polyurethane applications, a variety of polyols has been selected in industry, but relatively a few isocyanate has been used (Zhang et al., 2013). However, a demand of green monomers excessively increases to replace petrochemical polyol, and then vegetable oils such as soybean oil and castor oil have been focused (Veronese et al., 2011; Zhang et al., 2014). Typically, ring-opening of ESO's epoxides is commonly used to synthesize polyols from soybean oils through using alcohols, inorganic acids, and hydrogenation (Zhang et al., 2013).

Bio-based polyurethanes were derived from a polyol mixture of ESO and isopropanol amine (Miao et al., 2013). Ester groups and epoxy groups of ESO were reacted with amino groups of isopropanol to produce hydroxyl groups onto fatty acids of ESO. The polyol mixture was waxy at room temperature, and it showed a glass transition temperature at 38.32 °C and melted at 46.45 °C. The synthesized polyol had 317 mg KOH/g hydroxyl number; commercial petroleum-based polyols for rigid polyurethanes generally need to contain a 300-650 mg KOH/g of hydroxyl number range (Veronese et al., 2011). The polyol mixture was cured with 1,6-diisocyanatohexance including 1,3-propanediol as a chain extender to generate polyurethanes. The synthesized polyurethane exhibited tensile strengths in the range from 9.3 to 22.89 MPa and elongations at break in the range from 116.97 to 168.61 % as the polyurethane contained different amounts of the chain extender; high contents of the chain extender in the polyurethanes definitely improved mechanical strengths such as tensile and yield strength. The synthesized polyurethanes had glass transition temperatures in a range of 24-29 °C, and thermal degradation temperatures in TGA analysis (5 % weight loss) ranged from 240 to 255 °C.

An oxirane of ESO were converted to a hydroxyl group with a various functional groups such as a methoxy, a bromide, a chloride, and hydrogen (Guo et al., 2000). The methoxylated soy polyol was liquid at room temperature, and the other three soy polyol formed waxes at room

temperature. The brominated soy polyol showed the highest viscosity, whereas hydrogenated soy polyol had the lowest viscosity. Relate to the research, soybean oil-based polyurethanes were synthesized by the four polyols with commercial isocyanates (Z. S. Petrovic et al., 2000). The highest crosslink density between polyols and isocyanates were shown in polyurethanes with brominated polyol. However, the polyurethanes with brominated polyols exhibited the lowest thermal stability followed by polyurethanes with chlorinated polyols, whereas methoxy and hydrogenated polyol-containing polyurethanes had high thermal stability. Obviously low tensile strength and Young's modulus were found at polyurethanes with hydrogenated polyol in compared with other three polyol containing polyurethanes.

Our lab previously succeeded in synthesis dihydroxyl soybean oil (DSO) as a soy polyol from commercial ESO with perchloric acid in tetrahydrofuran/water solution, and we have successfully produced novel soybean oil-based pressure sensitive adhesives (PSA) using DSO as a PSA additive to improve tackiness and softness (Ahn et al., 2011a; Ahn et al., 2013; Ahn et al., 2011b). Firstly, copolymers of ESO and DSO in the presence of phosphoric acid showed a potential for PSA applications, and the chemistry was confirmed by a simple fatty acid model, which included epoxides and diols from oleic acid methyl ester (Ahn et al., 2011b). The research found that phosphate ester crosslinks and ether crosslinks were generated by ring-opening polymerization of epoxides and hydroxyl groups. In the next research, synthesis PSA from copolymerization of ESO and DSO was optimized to be comparable with commercial PSAs such as Scotch Magic Tape and Post-it. The optimized ESO/DSO (weight ratios of 1.5:1) PSA on aluminum foil carriers showed a peel strength approximately 2.2 N cm^{-1} while Scotch Magic Tape and Post-it had 2.5 and 0.55 N cm^{-1}. In addition, the ESO/DSO PSAs were clearly removed from adherend indicating a potential of reusable PSA applications. Also, the ESO/DSO PSAs

were thermally stable (no melting points existed) and optically transparent (showed a similar optical transmittance of micro cover glass). The ESO/DSO PSAs were advanced by an addition of rosin ester with photoinitiated copolymerization process (Ahn et al., 2013). The UV-cured PSA (ESO:DSO:rosin ester (weight ratio of 1:1:0.7)) on polyethylene terephthalate (PET) carrier showed similar peel strengths of Scotch Magic Tape, and the PSA had approximately twice higher peel strength than that of Scotch Magic Tape when the PSA was applied on aluminum foil as a carrier. In addition, the PSA on PET carrier exhibited extensively higher shear tack time (>30000 min) than that of commercial PSA such as Scotch Magic Tape (10000 min) and Post-it (1 min) when 1 kg of weight applied on the shear tack tests.

Plasticizer applications

Plasticizers are importantly used as additives in polymer industries to increase flexibility and processability of polymers by reducing the glass transition temperature (Adeodato Vieira et al., 2011; Sejidov et al., 2005). Fracture resistance of polymers is also improved by plasticizers effect, whereas tension and hardness of polymers are reduced (Rosen, 1993). For productions of bio-based polymers films and coating, plasticizers also have the significant role in the polymer matrix to improve flexibility and handling of films, and reduce pores and cracks in the polymer (Garcia et al., 2000). In addition, natural-based plasticizers have received attention from both bio-based polymers and petrochemical-based polymers because of their low toxicity and migration (Adeodato Vieira et al., 2011). Epoxidized triglycerides plant oils such as soybean oil, linseed oil, castor oil, sunflower oil, and fatty acids esters are mainly included in the natural-based plasticizers (Baltacioglu and Balkose, 1999). Vieira et al. defined that plasticizers could be either external or internal. External plasticizers have interaction with polymer chains without chemical bonds, so they can be removed by evaporation, migration or extraction (Adeodato

Vieira et al., 2011), Otherwise, internal plasticizers are performed as a part of the polymer chain through copolymerization or reaction with the other monomer of the original polymer (Frados, 1976). In addition, generally bulky structures of internal plasticizers provide steric hindrances to polymers, then the polymer matrix has more space instead of closed polymer chains (Adeodato Vieira et al., 2011).

ESO was studied as a plasticizer to improve the flexibility of poly(lactic acid) (PLA) with a simple single-step processing system (Vijayarajan et al., 2014). PLA is one of the common biodegradable polymers since it is derived from agricultural resources such as corn and sugar beets (Drumright et al., 2000). In addition, PLA has been attractive materials to substitute petroleum-based polymers due to its high modulus, thermal plasticity, low aroma permeability, and easy processing (Lee et al., 2008; Pilla et al., 2008). Although PLA has a lot of interests to commercial polymer products, its applications for flexible goods such as sheets and films are limited due to the brittleness nature of PLA (Afrifah and Matuana, 2010; Martino et al., 2009; Schreck and Hillmyer, 2007). In order to improve flexibility of PLA, plasticizer additions into PLA blending have been studied, but the majority of plasticizers are petroleum-based materials (Robertson et al., 2010). From Vijayarajan's research, ESO and PLA were well blended and incorporated by the single-step processing system, which is an extruder and a peristaltic injector pump. The synthesized PLA showed that ductility increased from 4 to 50 % as ESO content in the PLA blend increased from 0 to 15 weight %. However, tensile strength and modulus, and glass transition temperature of the synthesized PLA decreased as ESO contents increased in the PLA blend. Nevertheless, Impact strength of PLA with 15 weight % of ESO had over three times higher than that of PLA without ESO content. The enhanced impact strength was caused by a dissipation of fracture energy from the dispersed ESO phase in the PLA matrix, and the

dispersions of ESO were observed in SEM images in the research. ESO acted as plasticizer into the PLA matrix to increase flexibility of the PLA, and miscibility of ESO into the PLA retarded fracture propagation following an increase in impact strength.

Poly (3-hydroxybutyrate-co-3-hydroxyvalerate) (PHBV), which is a biodegradable thermoplastic from bacterial fermentation method for medical applications, was blended with several biodegradable plasticizers such as soybean oil (SO), ESO, dibutyl phthalate(DBP), and triethyl citrate(TCE) (Choi and Park, 2004). In the results of glass transition temperature, elongation at break, and impact strength, DBP and TCE plasticized PHBV showed better efficiency of plasticizers than ESO and SO plasticized PHBV. The low efficiency of triglycerides-based plasticizers could be caused by their bulky structures and higher molecular weight (814.3 of SO and 872.2 of ESO) in compared with low molecular weights of DBP and TCE (278.2 and 276.1). These results were also confirmed by solubility parameter, and polar and hydrogen components test, which indicated that those parameters of DBP and TCE were closer to parameters of PHBV than these of ESO and SO.

ESO was also used as a bio-based plasticizer to produce ethyl cellulose films (Yang et al., 2014). Ethyl cellulose (EC) is widely applied for pharmaceutical applications as a coating agent and an encapsulation due to its low cost and excellent film forming (Murtaza, 2012; Sogol and Ismaeil, 2011). However, EC is naturally brittle and has high glass transition temperature. From Yang et al., water vapor permeability of EC film was dramatically reduced by increases in ESO additions up to 30 % contents in the polymer. Oxygen permeability was also dropped by ESO additions. The low level water and oxygen permeability of ESO plasticized EC were results of hydrophobic nature and high molecular weight of ESO (Yang et al., 2014). However, elastic

modulus and tensile strength of EC/ESO films were extensively reduced as general plasticizers lead low mechanical strength and stiffness of polymers.

ESO also had been studied to replace petro-chemical plasticizers for polyvinyl chloride (PVC) (Bueno-Ferrer et al., 2010). PVC is commonly used in an wide range of commercial goods such as paints, coatings, films, medical devices, and food packaging. (Starnes, 2002). Phthalate derivatives are generally used as plasticizers for PVC productions, but the plasticizers cause hazards to human and environment (Rhee et al., 2002). Ferrer et al. gave attention to ESO as not only plasticizer but also stabilizer. The reaction of oxirane from ESO and hydrogen chloride from PVC thermal degradation can reinstate the released chlorine atoms into the original polymer, and the reaction helped PVC polymeric matrix to be stabilized (Parreira et al., 2002). From Ferrer et al., ESO had been successfully performed the role of plasticizer in PVC and stabilization of PVC, which was indicated by increases in of thermal degradation temperatures up to 20 °C as ESO content was 50 % of the PVC.

Bio-based coating and composite films

Mechanical and barrier properties of coating materials are required in order to achieve shelf life of both package and packaged product for packaging applications (Khwaldia et al., 2010). The mechanical properties generally include tensile and bending strength, elongation, and elastic modulus. The barrier properties include water vapor permeability and gas barrier properties such as oxygen, nitrogen, and carbon dioxide. Therefore, synthetic petroleum materials such as polyethylene (PE) and polyethylene phthalate (PET) are commonly layered with aluminum foil or deposited on Al_2O_3 in large scale packaging applications due to combination of excellent mechanical properties of the polymer and significant gas barrier properties of aluminum foil (Aulin et al., 2012). In order to meet desired properties of various

polymer applications, bio-plastics also can be blended, composited, or laminated with other renewable resources, petrochemical derivatives, or inorganic components (Siracusa et al., 2008; Tharanathan, 2003).

Since plastics are consisted of polymers and various chemicals such as additives, plasticizer, stabilizer, colourants etc., bio-plastic goods using 100 % renewable resources is not possible currently (Siracusa et al., 2008). Therefore, European Bioplastics defines that more than 50 % weights of renewable resources should be used to form bio-plastics. Bio-plastics could be comprised of either biodegradable plastics or bio-based plastics (Figure 2.2) (Siracusa et al., 2008; Tokiwa et al., 2009). From the definition of bio-plastics, several synthetic polymers from renewable resources are biodegradable such as starch, PLA, polyhydroxy butyrate (PHB), and cellulose. Otherwise, polycaprolactone (PCL) and polybutylene succinate (PBS) are also bio-plastics although they are derived from petrochemical resources because they are environmentally degraded by enzymes and microorganisms (Tokiwa et al., 2009). In addition, several bio-plastics from renewable resources are not biodegradable such as bio-polyethylene (PE), Nylon 9 (NY9), Nylon 11 (NY11), and acetyl cellulose (AcC), because the bio-mass monomers of the polymers could lose their natural biodegradability through chemical alteration such as polymerization (Siracusa et al., 2008).

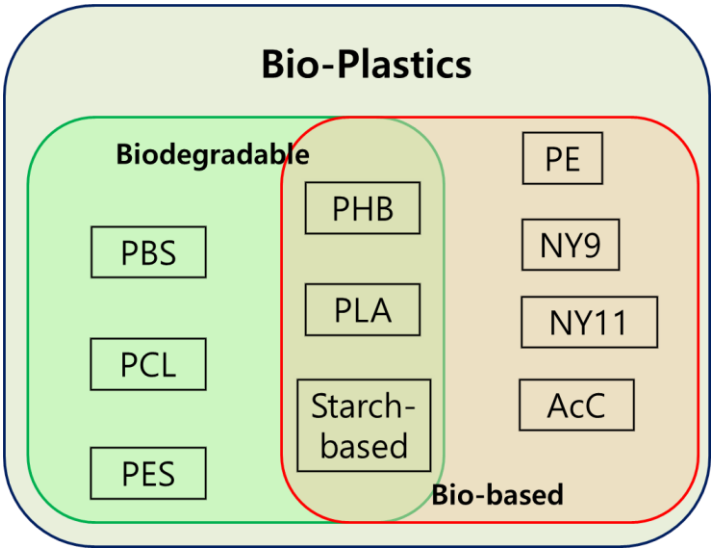

Figure 2.2: Two compositions of Bio-plastics: biodegradability and/or renewability (Tokiwa et al., 2009).

Plant oil-based coatings and composites

Bisphenol A-based epoxy resin is commonly used for coatings, paints, adhesives, and civil engineering applications due to its high tensile, bending, and compression strengths. However, the brittle nature of the epoxy resin causes low flexibility and impact strength. In addition, the high viscosity of the resin leads low processability (Czub, 2006). In research from Czub, ESO was used as a renewable diluent material to reduce the viscosity of the bisphenol A-base epoxy resin. Czub also defined that the diluent could be considered as an internal plasticizer due to their structure. From the results of the research, the viscosity of the epoxy resin was reduced by an increase in ESO addition, but 2-ethylhexyl-glycidyl ether as a commercial diluent more strongly cut down on the viscosity of the resin. In addition, obvious plasticizer effects of ESO were obtained by mechanical tests. From the mechanical properties data, tensile strengths and modulus, compression strength, and hardness were reduced to approximately 10 % of the pure epoxy resin's properties while ESO was applied up to 54 % of the weight of the resin

mixture. Otherwise, elongations at break and impact strengths of the epoxy resin showed a tendency of improvements as ESO contents increased in the resin. Similar results were also reported from other research (Gupta et al., 2011).

Functionalized soybean oil such as AESO, maleinized acrylated epoxidized soybean oil (MAESO), and soybean oil pentaerythritol maleates (SOPERMA) were respectively combined with styrene to become polymer matrix, and clay nanocomposites were prepared from the soybean oil-based polymers (Lu et al., 2004). From Lu et al., the monomers showed better miscibility with nanoclay in compared with unmodified soybean oil because high solubility parameter and polarity were caused by the chemical modification of soybean oil. The bending modulus and storage modulus were increased by nanoclay additions, but thermal decomposition temperatures of the composites were not significantly improved. Uyama et al. also researched on ESO and nanoclay composites, and they confirmed well dispersed silicate layers of nanoclay in the ESO polymer matrix through using TEM image (Uyama et al., 2003). Liu el al. studied to increase reinforcing ability of nanoclay in ESO polymer through using triethylenetetramine (TETA) as a curing agent (Z. Liu et al., 2005). From the results of the research, tensile strength, storage modulus, and thermal decomposition temperatures were increased as nanoclay contents were increased in the composites, whereas glass transition temperatures were not significantly changed by nanoclay contents.

Plant oil derivatives have been studied incorporation with traditional reinforcements such as glass and carbon fiber to improve strengths and rigidities (Z. S. Liu et al., 2004; Rangasai et al., 2014; Thulasiraman et al., 2009). Liu et al. reported glass and carbon fibers reinforced composites of ESO and epoxy resin using curing agents, which demonstrated better mechanical properties such as bending modulus and strength. In addition, a combination of glass and carbon

fiber in the composites leaded higher strength of the composites than that of single fiber in the composites (Z. S. Liu et al., 2004). Thulasiraman et al. prepared composites from chlorinated soy epoxy resin as a soybean oil derivative and glass fiber with m-phenylene diamine as a curing agent. The modified epoxy resin/glass fiber composites showed an excellent tensile strength (248-299 MPa) and a bending strength (346-379 MPa). Moreover, the impact strength and the fracture toughness of the composites were enhanced by increases in chlorinated soy epoxy resin compositions.

Other renewable raw materials

Proteins have been researched to form into coatings, and proteins are applicable to coatings for paper packaging, and the protein coatings have been derived from milk protein such as casein, wheat gluten, whey protein, and soy protein (Khwaldia et al., 2010). The protein-derived coatings have low oxygen permeability at low to intermediate relative humidity (Khwaldia et al., 2010). However, a water vapor permeability of the protein-derived coatings is poor since they are naturally hydrophilic (Avenabustillos and Krochta, 1993). Soy protein isolate (SPI) and nanoclay composite coatings were derived by formaldehyde as crosslinking agent (Rhim, Lee et al., 2006). The SPI/nanoclay coatings exhibited enhancement of mechanical and water vapor barrier properties. However, the crosslinking agent residues in the coating should be concerned because of the possible toxicity of formaldehyde (Khwaldia et al., 2010). Polyphosphate filler was also blended into soy protein composites to improve mechanical properties and water resistance (Otaigbe and Adams, 1997). Rhim et al. researched on multilayer films of SPA and PLA to enhance both water resistance and oxygen barrier properties since PLA had low water vapor permeability with high strength and modulus (Rhim, Mohanty et al., 2006). The SPI/PLA multilayer films were consisted of SPI inner layer and PLA outer layer, and its

mechanical properties were comparable to commercial polymers such as low density polyethylene (LDPE) and high density polyethylene (HDPE).

Polysaccharides also have been studied as coating materials due to their excellent gas, aroma, and lipid barrier properties (Khwaldia et al., 2010), but they exhibit poor water vapor barrier properties because of their hydrophilic nature (Kester and Fennema, 1986). Chitosan, a natural polysaccharide, can be film forming, and it shows high flexibility and tear strength (Khwaldia et al., 2010). In addition, chitosan exhibits good oxygen barrier properties because its hydrogen bond between the molecular chains (Gallstedt and Hedenqvist, 2004). Currently, chitosan and nanoclay multilayer coated with PLA films exhibited higher oxygen barrier properties PET, a commercial synthetic plastic, at 20 and 50 % relative humidity, but in compared with uncoated PLA films, water vapor permeability of the chitosan and nanoclay coatings reduced by only 20 % when 70 bilayers of the chitosan and nanoclay coatings were applied (Svagan et al., 2012).

Hybrid films of nano-fibrillated cellulose (NFC) and nanoclay were studied to replace petroleum-based packaging materials such as PE and PET (Aulin et al., 2012). The hybrid film exhibited high oxygen barrier properties due to deposited vermiculite nanoplatelets as nanoclay. In addition, water vapor permeability of the hybrid film was significantly reduced at 50 and 80 % relative humidity in compared with pure NFC. Furthermore, the hybrid film had excellent tensile strength about 250 MPa and high Yong's modulus about 14.2 GPa due to tough and flexible properties of NFC. However, homogenization of NFC and nanoclay was followed by high pressure stirring for 24 hour to prepare the hybrid film. The long-time step of preparation films could not be suitable for large scaling.

Ring-opening cationic photopolymerization

Mechanism

Ring-opening cationic photopolymerization of epoxides and epoxides, and also epoxides and alcohols have been studied (Chiang and Hsieh, 2006; Crivello and Liu, 2000; Decker et al., 2001; Dillman and Jessop, 2013; Voytekunas et al., 2008). Shown in Figure 2.3 (eq 1) (Crivello and Liu, 2000), diaryliodonium salts as a photoinitiator formed aryliodine radical cation and aryl cation under high intensity of UV irradiation which is most effective at 210-350 nm wavelengths (Cho et al., 2003). Strong Bronsted acid, HX, is generated by the monomer or impurities, R-H (eq 2). Epoxide is protonated by the Bronsted acid (eq 3). Since the Bronsted acid, $HSbF_6$ is very powerful acid, Crivello and Liu expected that the three rate constants, k_1, k_2, and k_3 were large due to the initiation steps had a low activation energy. In propagation steps of epoxide ring-opening by epoxide (eq 4 and 5), the protonated epoxide is opened by nucleophilic attack of the other epoxide, and a hydroxyl is generated by the ring-opening of the epoxide (eq 4). Then, the next propagation step generates ether crosslinks and new protonated epoxide in the polymer chain (eq 5) until protonated epoxides survive. However, eq 5 is strongly limited by the structure of the epoxy monomer because the reaction is affected by steric, electronic, and stereochemical effects (Crivello and Linzer, 1998). However, propagation steps of epoxide ring-opening by hydroxyl are finished at two steps (eq 6 and 7). In eq 6, the protonated epoxide is opened by the nucleophilic attack of the hydroxyl group, and then it forms protonated ether. The protonated ether is deprotonated by the nucleophilic attack of the other epoxide, and the proton is transferred to the attacking epoxide which becomes a new propagation starting monomer. Therefore, the propagation of the first polymer chain is stopped at eq 7 as a termination step. Crivello and his research team previously confirmed that additions of alcohol leaded an acceleration of

photoinitiated cationic polymerization of epoxides since eq 6 and 7 had less steric hindrance effects at the reaction than that of eq 4 and 5 (Crivello et al., 1986).

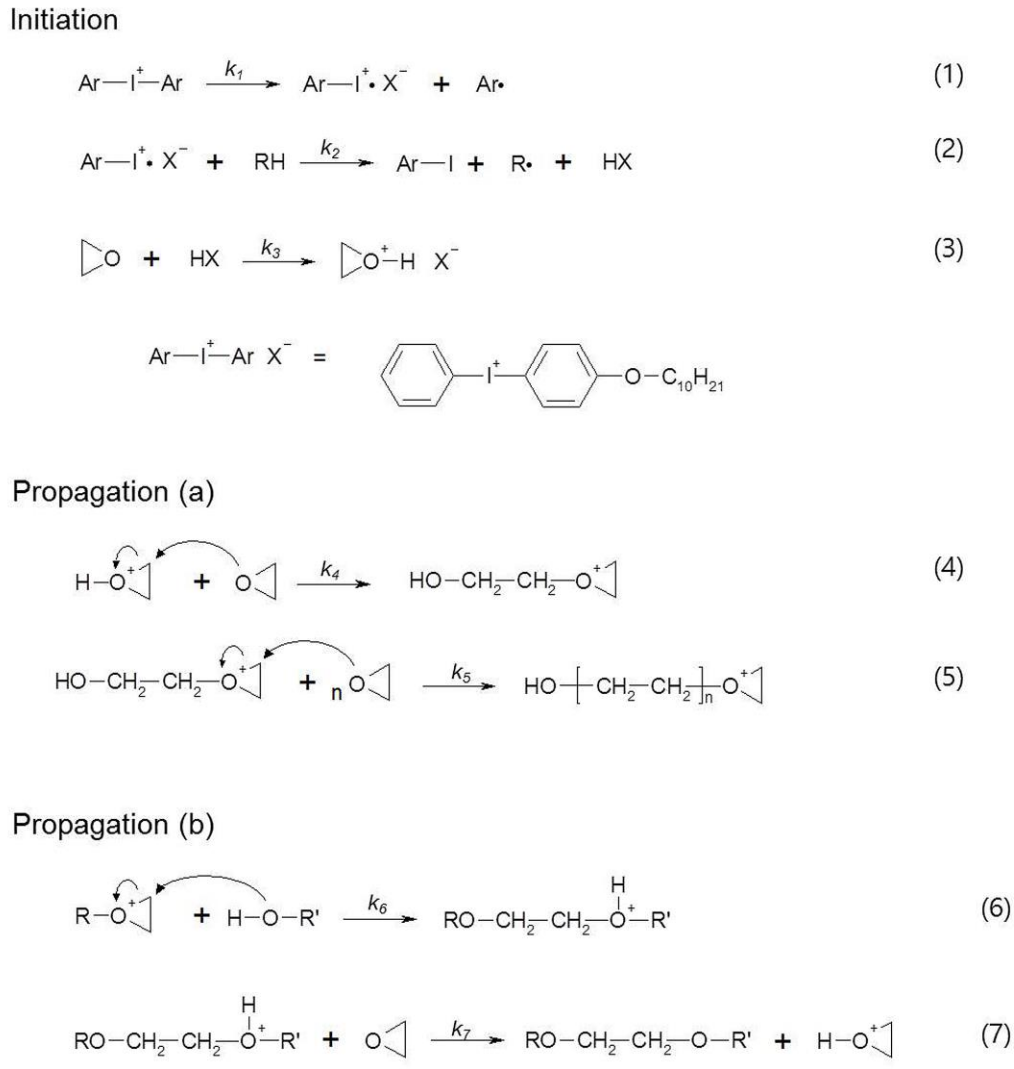

Figure 2.3: Photoinitiated cationic polymerization of epoxide and alcohol (Crivello and Liu, 2000). Propagation (a) is ring-opening polymerization by attacks of epoxides, and propagation (b) is ring-opening polymerization by attacks of alcohol.

Characteristics

In comparison to free radical photopolymerization which is mainly based on acrylates, cationic photopolymerization of epoxy offers several advantages such as low shrinkage, uninhibited process in oxygen, and enabled post-polymerization after UV exposure stopped (dark-curing behavior) (Sipani and Scranton, 2003; Voytekunas et al., 2008). However, free-radical photopolymerization has been more widely used in UV curing polymer market (Cho and Hong, 2004). The reasons are probably the characteristics of cationic photopolymerization, which are the lower curing speed and environmental sensitivities such as temperature and moisture (Fouassier and Rabek, 1993). Golaz et al. studied cationic photopolymerization of ECHM as a cycloaliphatic epoxy resin to examine effects from UV intensity, temperature and post-polymerization at high temperatures (Golaz et al., 2012). In the research, photo-differential scanning calorimetry (p-DSC) was used to obtain conversions of the epoxy versus time at various temperatures and UV intensities. In addition, peaks of storage and loss modulus, and Tan δ were clearly shifted to higher temperatures after post-polymerization was performed at 200 °C for 2 hours. As the results, higher temperature and UV intensity leaded high conversion of the epoxy, and the glass transition temperature and the storage modulus of ECHM polymer were increased by the thermal post-polymerization. The result of temperature effects to conversion rates was also reported by other research (Voytekunas et al., 2008). Voytekunas et al. used two cycloaliphatic epoxy monomers to observe an influence of chemical structures of monomers (Figure 2.4), and Bis-(3,4-epoxycyclohexyl) adipate showed two times faster polymerization in compared with polymerization of ECHM. The result could be explained by that more space of the two carboxylate structure provided better flexibility on the structure in compare with the short and tight structure of ECHM (Voytekunas et al., 2008).

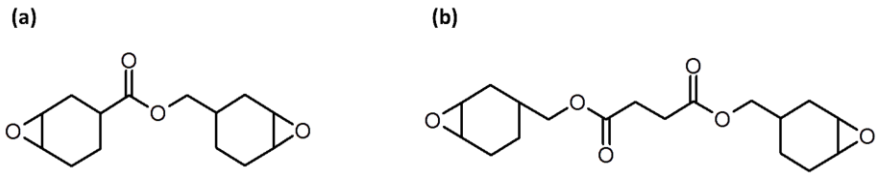

Figure 2.4: Structures of (a) 3,4-epoxycyclohexylmethyl-3,4-epoxycyclohexane carboxylate (ECHM), and (b) Bis-(3,4-epoxycyclohexyl) adipate (Voytekunas et al., 2008).

Chapter 3 - Materials and methods

Raw materials

Epoxidized soybean oil (ESO) (Scientific Polymer Products, Inc., Ontario, NY) was used as a bio-based monomer of the coating material and a starting material of dihydroxyl soybean oil (DSO). 3,4-epoxycyclohexylmethyl-3,4-epoxycyclohexanecarboxylate (ECHM) (Sigma-Aldrich, St. Louis, MO) was used as a petrochemical-based monomer of the coating material. PC-2506 (Polyset, Mechanicville, NY; [4-(2-hydroxyl-1-tetradecyloxy)-phenyl] phenyliodonium hexafluoroantimonate) was used as a photoinitiator of cationic photopolymerization. Structures of these materials are shown in Figure 3.1.

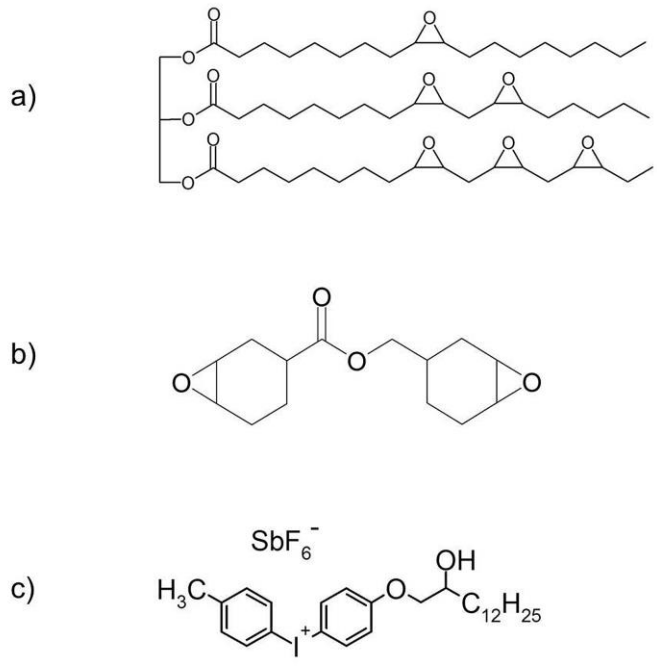

Figure 3.1: Structures of (a) ESO, (b) ECHM, and (c) PC-2506.

Dihydroxyl soybean oil synthesis

ESO (40 g, 40 mmol) was dissolved in dissolved in 60 mL of tetrahydrofuran (THF)/water (40 mL: 20 mL), and 1.5 % (volume of ESO) of perchloric acid was gently added. Hydroxylation of ESO was performed for 5 hours at room temperature with magnetically stirring. After the reaction was completed, the aqueous layer of the mixture was separated and removed from the organic layer in a separatory funnel by adding 60 mL of ethyl acetate. Then, 60 mL of water was added into the organic layer in the separatory funnel to remove perchloric acid residues, and the perchloric acid in the aqueous layer was removed from the funnel. The water washing steps were repeated at least three times until pH of the aqueous layer reached between 8 and 9 after adding 5~6 ml of saturated sodium bicarbonate for neutralization of the mixture. The solvent in the organic layer was removed by a rotary evaporator with a tap vacuum at 40 °C of water bath, and then the organic layer was dried under high vacuum with a rotary evaporator at 80 °C of water bath to remove remaining water residues. The synthesized DSO was transparent and light yellowish, and the chemical structure of DSO was described (Figure 3.2).

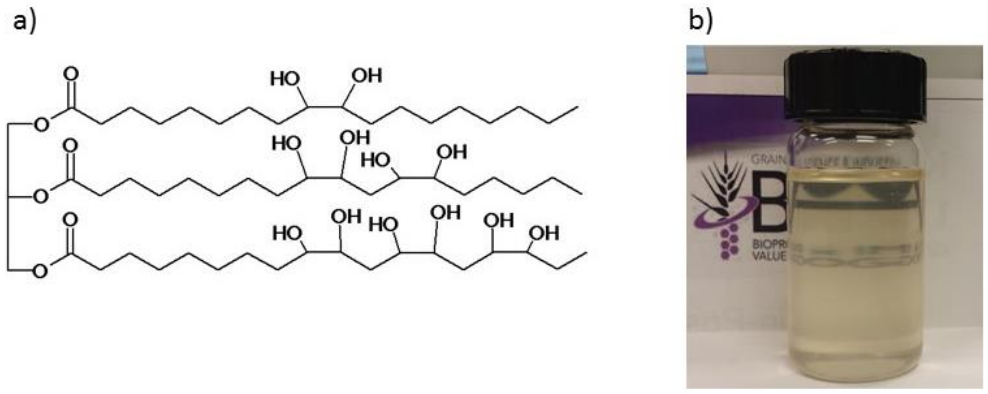

Figure 3.2: (a) a structure of DSO and (b) picture of DSO product.

Preparation of UV-cured films

From our previous research, UV-curable pressure sensitive adhesives of ESO, DSO, and rosin tackifier were studied using 3 wt% photoinitiator in ESO (Ahn et al., 2013). In ECHM, 3 wt% of photoinitiator was found optimal for photopolymerization of the cycloaliphatic diepoxide resin (Voytekunas et al., 2008), so we used 3 wt% photoinitiator (based on epoxy monomers) for all film preparations. UV-curable copolymer films were prepared at various ratios of ESO and DSO and ECHM and DSO monomers to characterize mechanical, viscoelastic, thermal, and optical transparent properties for coating applications. ESO and DSO were mixed at weight ratios of 1:0.1, 1:0.15, and 1:0.2 (Table 3.1). The mixture was heated and mixed using a heat gun and a vortex mixer. Subsequently, 3 wt% (weight of ESO) cationic photoinitiator PC-2506 was added to the mixture and mixed well using the vortex mixer and a sonicator. Approximately 8 g of the mixture was spread over a glass plate (25.4 cm by 15.24 cm) as a substrate using a wire wound rod (Figure 3.3) (#90; ChemInstruments, Fairfield, OH). The spread mixture was passed twice at a conveyor rate of 7 ft min^{-1} (radiation dose of 1.7 to 1.8 J cm^{-2}) through a F300 UV system (1.8 kW, 6-inch (300 W in^{-1}) lamps) equipped with a LC6B benchtop conveyor (Figure 3.4) (Fusion UV system, Gaithersburg, MD). The UV lamp was 10 cm above the conveyor belt. To obtain free-standing films, appropriate thicknesses of the UV-cured films were from 0.13 mm to 0.15mm. ECHM/DSO films were prepared similarly at ECHM/DSO weight ratios of 1:1, 1:1.18, and 1:1.43 with three UV passes at a conveyor rate of 10 ft min^{-1} (Table 3.1). The UV-cured films could not be detached from the glass substrate without cohesion failure right after UV-curing. Based on our preliminary test for making free-standing films, 3hours is just enough to peel off the films from glass substrates without any cohesion failure. Therefore, all UV-cured films were peeled from the glass plates 3 hours after the completion of UV curing, then films

were stored in the dark for 3 hours, 1 day, 5 days, 10 days, 1 month, and 2 months at room temperature to obtain samples for shelf life and dark-curing effect studies. All composition of the UV-cured films and their bio-contents are summarized in Table 3.1.

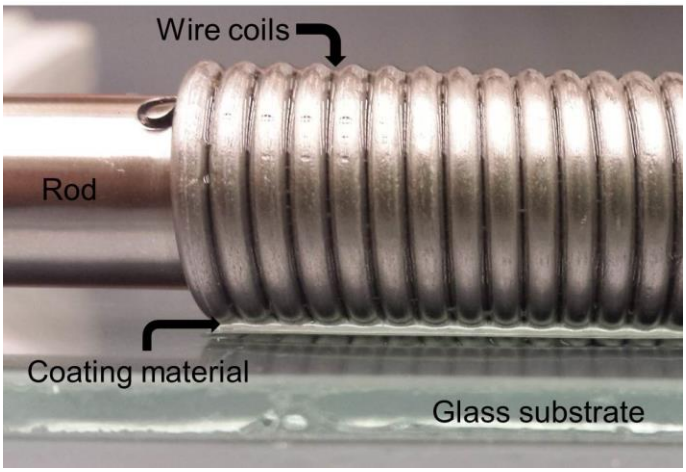

Figure 3.3: Scheme of wire wound rod and apply to spread coating material.

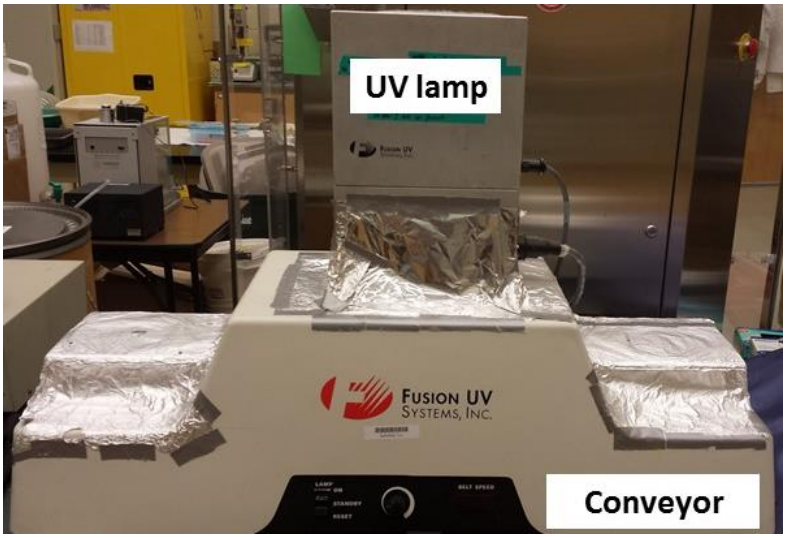

Figure 3.4: UV lamp is applied on the top of the conveyor system.

Table 3.1: Resins composition and bio-contents at weight % for UV-cured films.

Sample	ESO (%)	ECHM (%)	DSO (%)	Photoinitiator (%)	Bio-contents (%)
ESO:DSO(1:0.1)	88.50		8.85	2.65	97.35
ESO:DSO(1:0.15)	84.75		12.71	2.54	97.46
ESO:DSO(1:0.2)	81.30		16.26	2.44	97.56
ECHM:DSO(1:1)		49.26	49.26	1.48	49.26
ECHM:DSO(1:1.18)		45.25	53.39	1.36	53.39
ECHM:DSO(1:1.43)		40.65	58.13	1.22	58.13

Fourier transform infrared (FTIR) spectroscopy

Perkin-Elmer Spectrum 400 FTIR spectroscopy (Waltham, MA) was used to verify cationic ring-opening photopolymerization of the resins and the dark-curing effect by comparing functional groups such as hydroxyl, epoxy, and ether groups. Data for non-cured resin blends and UV-cured films at 3 hours and 10 days after curing for both ESO/DSO (w/w ratio of 1:0.15) and ECHM/DSO (w/w ratio of 1:1.18) films were collected.

Characterize properties of UV-cured films

Thermal properties

A differential scanning calorimetry (DSC) (TA DSC Q200, New Castle, DE) and a thermogravimetric analyzer (TGA) (PerkinElmer Pyris 1 TGA, Norwalk, CT) were used to obtain thermal properties of the UV-cured films to determine thermal stability of the coating materials. All UV-cured samples for thermal analysis were measured within 30 min after UV curing to reduce dark-curing effect. UV-cured and non-cured ESO/DSO (w/w ratio of 1:0.15) and ECHM/DSO (w/w ratio of 1:1.18) films and resins, as well as both monomers, were measured. Thermal transitions (glass transition temperature, T_g, and melting temperature, T_m) and heat of copolymerization (ΔH) were obtained. All cured and non-cured samples for DSC

contained 3 wt% (weight of ECHM or ESO) photoinitiator. Approximately 5 to 7 mg of the sample was heated from -50 to 250 °C at a rate of 10 °C min^{-1} under a nitrogen environment in a hermetic pan. Conventional Modulated Differential Scanning Calorimetry (MDSC) mode was used to determine accurate T_g of ESO/DSO and ECHM/DSO cured films from -50 to 200 °C at a rate of 3 °C min^{-1}. Thermal decomposition characteristics of 1:0.15 w/w ratio of ESO/DSO and a 1:1.18 w/w ratio of ECHM/DSO UV-cured samples were obtained using TGA and compared with the decomposition characteristics of ESO and ECHM UV-cured homopolymers, respectively, and 6 to 8 mg of each sample was heated from 30 to 650 °C at a rate of 20 °C min^{-1} under a nitrogen atmosphere.

Viscoelastic behaviors

To obtain viscoelastic properties of the UV-cured films at all weight ratios, dynamic mechanical analysis (DMA) was performed with a TA DMA Q800 (New Castle, DE) with a tension/film clamp using rectangular specimens approximately 2 cm long, 1.27 cm wide, and 0.13 to 0.15mm thick. The measurements were performed at a frequency of 1Hz, a constant amplitude of 15 μm, and a heating range of -50 to 150 °C with 10 °C min^{-1} increments. T_g was determined at maximum tangent delta peak, and crosslink density (ν_e) and molecular weight between crosslink (M_c) were calculated from an elastic modulus (E') based on the rubbery plateau region at least 50 °C above T_g (Asif et al., 2005; Chen et al., 2010; Rao and Palanisamy, 2008).

Mechanical properties

Tensile strength and elongation at break of UV-cured films at all weight ratios were measured according to ASTM D882-12. The UV-cured films were cropped to 20.32 cm long,

1.27 cm wide, and 0.13 to 0.15 mm thick according to ASTM D6287-09 using a dual-blade shear cutter (Figure 3.5) (JDC Precision Cutter 10", Thwing-Albert Instrument Company, West Berlin, NJ). A strip of the film was applied on a tensile tester (TT-1100, ChemInstruments, Fairfield, OH) with 12.7 cm of initial grip separation and a rate of grip separation of 2.54 cm min^{-1}. The mechanical test was conducted at various times (1, 5, and 10 days, and 1 and 2 months) after UV curing to evaluate shelf life of the bio-based films.

Figure 3.5: Dual-blade shear cutter

Optical transmittance

Optical transparencies of UV-cured ESO/DSO (w/w ratio of 1:0.15) and ECHM/DSO (w/w ratio of 1:1.18) films were measured with a UV-visible spectrometer (Hewlett-Packard 8453) with a wavelength range of 200 to 900 nm. In addition, transmittance data for a micro cover glass and a polyethylene terephthalate (PET) film were also obtained to be compared with the UV-cured films. The thickness of loading samples was 0.14 mm for ESO/DSO and ECHM/DSO films, 0.04 mm for the PET film, and 0.91 mm for the micro cover glass.

Water uptake properties

Water absorptions of the UV-cured films containing the highest hydroxyl groups such as ESO/DSO (w/w ratio of 1:0.2) and ECHM/DSO (w/w ratio of 1:1.43) films were estimated according to 24 hours immersion test of ASTM D570-98. The loading samples were 0.14 to 0.15 mm thick, and 2.54 cm long and wide. The samples had been soaked in distilled water at 22 °C for 24 hours, and wet weight of the samples were immediately measured after the surfaces of the samples were gently wiped using Kimwipes.

Chapter 4 - Results and discussion

Photoinitiated cationic polymerization of epoxy monomers

FTIR spectra were obtained to confirm functional groups of ESO/DSO and ECHM/DSO UV-cured films before and after photopolymerization (Figure 4.1 and 4.2). Epoxy peaks at 825 cm^{-1}, triglycerides at 1740 cm^{-1}, and alcohol bands around 3450 cm^{-1} were detected in the non-cured ESO/DSO curve (Figure 4.1). After 3hours of UV curing, the disappearance of the epoxy peak at 825 cm^{-1} and the appearance of an ether peak at 1075 cm^{-1} indicates that the reaction was completed for the polymerization of ESO and DSO (w/w ratio of 1:0.15) (Lligadas et al., 2006) (Figure 4.1). For ECHM and DSO (w/w ratio of 1:1.18), the reaction was not fully complete in 3 hours, which was confirmed by the remaining small epoxy peak at 790 $cm^{-1}$and the increment of the ether peak at 1070 cm^{-1} after 10 days (Figure 4.2).

The crosslinking reaction of epoxy and alcohol leads the termination of chain propagation and the active center transferring from the polymer chain (Figure 2.3, propagation (b)). In addition, the crosslinking reaction with alcohol was dominant in ECHM/DSO copolymer because the ECHM/DSO resins contained more alcohol groups than the ESO/DSO systems. Therefore, the longer time for the post-polymerization of ECHM/DSO copolymer could be caused by the new protonated epoxide monomers during the active center transferring. The increased alcohol bands around 3450 cm^{-1} after curing of both ESO/DSO and ECHM/DSO copolymers were due to the newly generated hydroxyl groups from the epoxy ring-opening polymerizations.

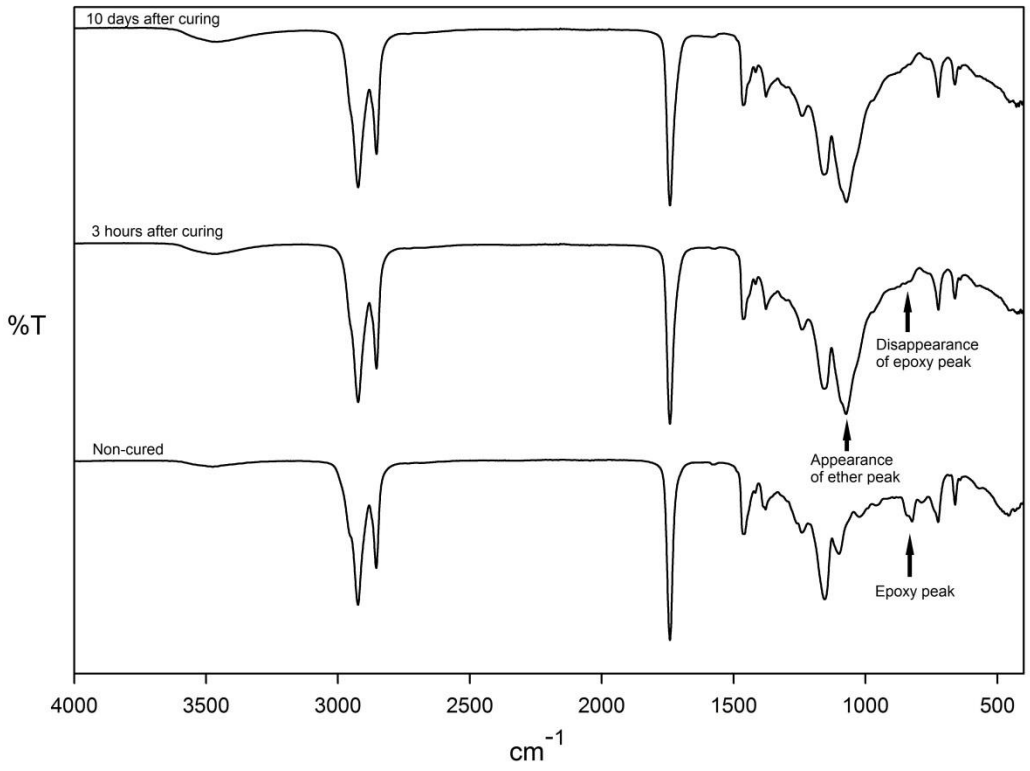

Figure 4.1: FTIR of ESO/DSO (weight ratio of 1:0.15) resin before UV curing, 3hours after UV curing, and 10days after UV curing.

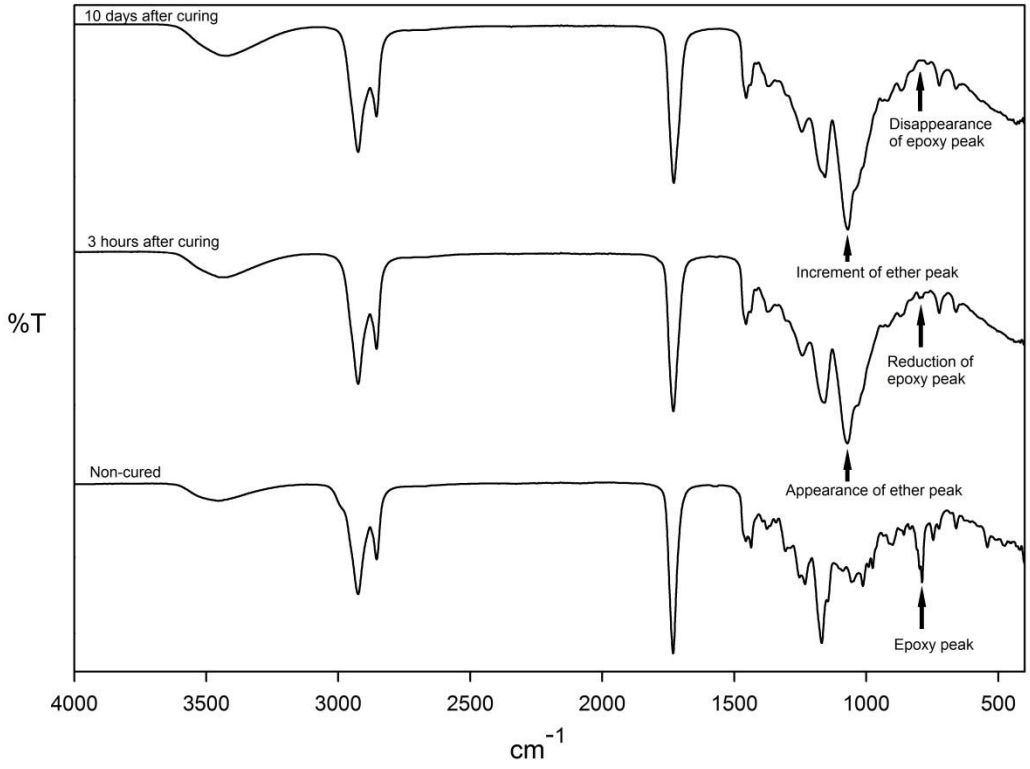

Figure 4.2: FTIR of ECHM/DSO (weight ratio of 1:18) resin before UV curing, 3hours after UV curing, and 10days after UV curing.

Thermal analysis

ESO before UV curing had a small endothermic peak around -6 °C showing crystalline structures of epoxide triglycerides (Figure 4.3 a). The peak disappeared after UV curing because crystallization was impeded by crosslinking of ESO epoxides (Shibata et al., 2009) (Figure 4.3 b). ESO before curing also showed a curing peak at 182 °C with ΔH of 379.2 J g^{-1}, and the DSO before curing exhibited a small curing peak at 187 °C with ΔH of 24.88 J g^{-1}, indicating that a small portion of the epoxy groups did not fully react during DSO synthesis. The ESO after UV curing showed a shallow and broad exothermic peak at 134.81 °C with ΔH of 58.27 J g^{-1}, which

was caused mainly by the crosslinking reaction of residual epoxides because the heat from DSC contributed to the crosslinking reaction following an improvement in epoxides mobility (Voytekunas et al., 2008). Similarly, the ESO/DSO (w/w ratio of 1:0.15) after curing showed a curing peak at 136.13 °C with ΔH of 87.71 J g^{-1}, and both cured ECHM and cured ECHM/DSO (w/w ratio of 1:1.18) also exhibited a peak of heat curing at 125.64 °C with ΔH of 28.24 J g^{-1} and 77.07 °C with ΔH of 33.52 J g^{-1}, respectively.

The addition of DSO decreased the polymerization temperature of ESO but not ECHM. ESO and DSO have basically same backbone structures (i.e., triglyceride), and the rate of epoxy-epoxy polymerization is lower than the rate of epoxy-hydroxyl polymerization. The faster rate of epoxy-hydroxyl polymerization is explained by the less steric requirements for the nucleophilic attack by a hydroxyl in compared with the attack by an epoxide. Therefore, the polymerization temperature of ESO with DSO addition was reduced. However, the polymerization temperature of ECHM was not reduced by DSO addition, because ECHM could be easily polymerized itself due to its small steric hindrance of the less bulky structure in compared with a triglyceride. Therefore, DSO did not significantly affect a reduction of polymerization temperature of ECHM.

ESO and ESO/DSO showed larger ΔH than ECHM and ECHM/DSO. Ring-opening photopolymerization of ESO tended to have a lower degree of polymerization. The lower degree of crosslinking reaction of ESO could be due to epoxide steric hindrance from the bulky structure of ESO. The steric hindrance of the ESO was also considered a reason for the low degree of epoxy conversion in photoinitiated cationic polymerization (Decker et al., 2001). In compared with ESO/DSO, ECHM/DSO showed higher degree of polymerization under UV-curing from the DSC analysis although it had longer time of post-polymerization completion using the FTIR results. Absences of melting peaks and presences of exothermic curing peaks in

UV-cured films confirmed that soybean-derived coating materials were thermosetting polymers. The photoinitiator (PC2506) was successfully dissolved into the resins and joined in the polymerizations, because the melting and the thermal decomposition peaks at 98.9 °C and 224.1 °C disappeared in both before and after UV-curing samples.

T_g was determined at various weight ratios of both ESO/DSO and ECHM/DSO films through MDSC and DMA analysis (Table 4.1). The T_g from DMA was determined at peak loss factor (Tan δ) (Figure 4.5 a and 4.5 b), and that from DMA was approximately 20 °C higher than that from DSC because DMA and DSC determined T_g based on different mechanisms; however, both DMA and DSC showed the same tendency toward T_g of the films as affected by DSO. T_g decreased as DSO increased because DSO acted as a plasticizer in the polymer matrix. Compared with the ESO/DSO films, ECHM/DSO films had much higher T_g, because of the rigid backbone structure of ECHM and higher reactivity of the external epoxides.

Thermal degradation of the films was measured using TGA (Figure 4.4). All UV-cured ESO/DSO and ECHM/DSO films had similar thermal stabilities and degraded in the temperature range of 339 to 428 °C; however, the ECHM/DSO film became more thermally stable than ECHM alone. The degradation temperatures of cured-ECHM were observed at 339 °C for 5% weight loss and 408 °C for 50% weight loss, and the decomposition temperatures of the ECHM/DSO (w/w ratio of 1:1.18) increased to 356 °C for 5% weight loss and 428 °C for 50% weight loss.

Table 4.1: Glass transition temperatures of various weight ratios of ESO/DSO and ECHM/DSO based on MDSC and DMA analysis.

Monomer/ratio	MDSC T_g (°C)	DMA T_g (°C)	
	0 hours	3hours	10days
ESO:DSO(1:0.1)	-2.8	18.5	18.8
ESO:DSO(1:0.15)	-4.8	16.6	17.1
ESO:DSO(1:0.2)	-5.4	14.0	14.9
ECHM:DSO(1:1)	51.0	66.7	67.1
ECHM:DSO(1:1.18)	36.2	60.8	58.5
ECHM:DSO(1:1.43)	30.8	51.2	50.8

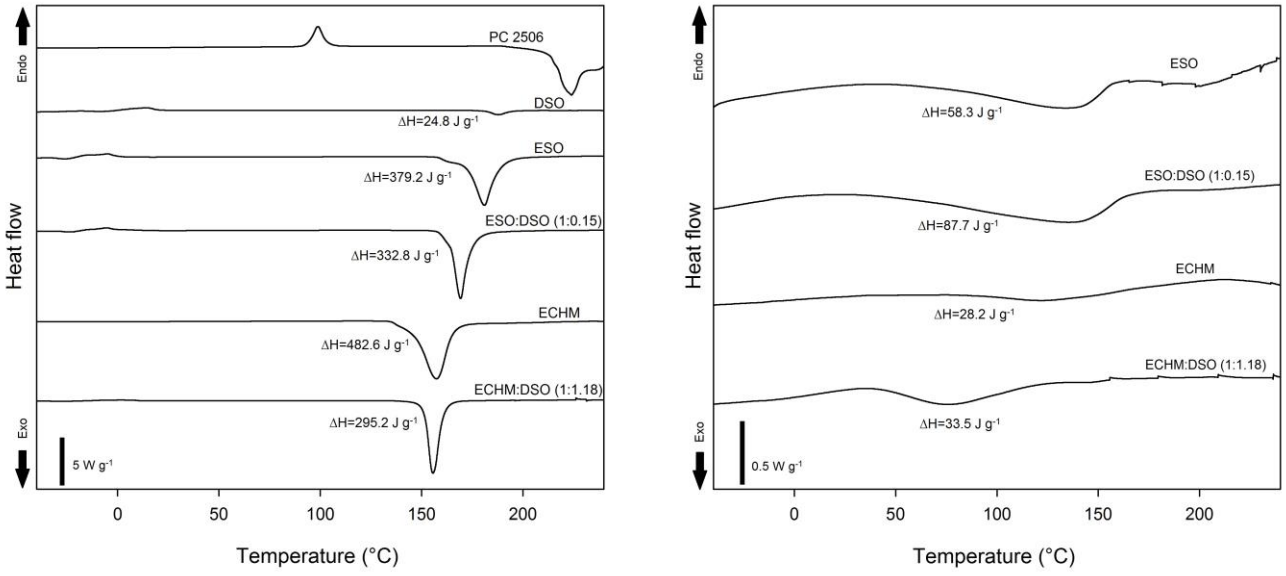

Figure 4.3: DSC thermograms of PC-2506, ESO, DSO, ESO/DSO (w/w ratio of 1:0.15), and ECHM/DSO (w/w ratio of 1:1.18) samples including the photoinitiator before (a) and after (b) UV curing.

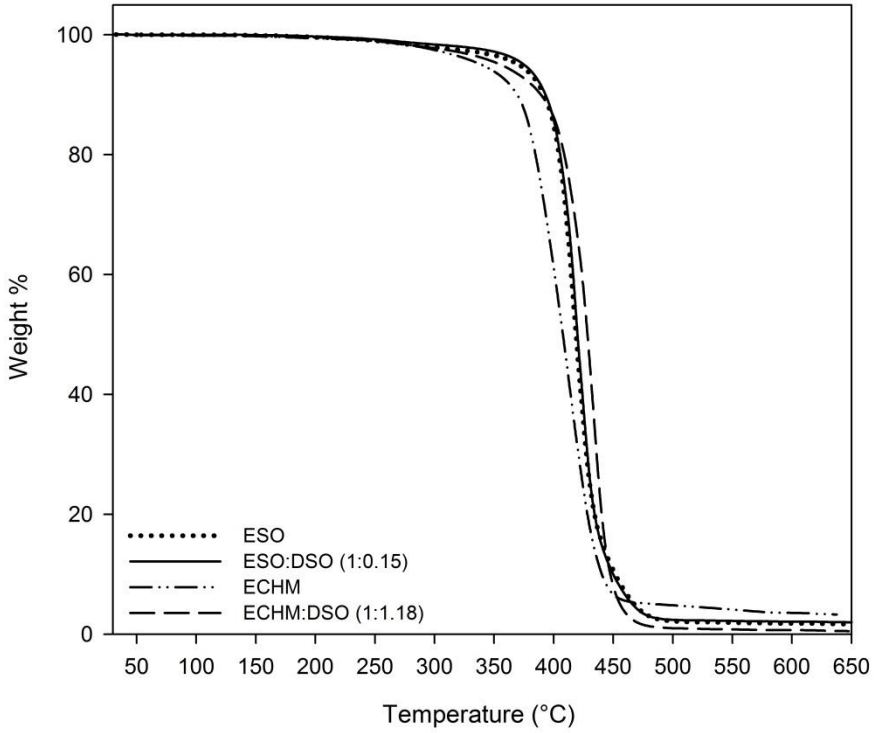

Figure 4.4: Thermal decomposition profiles of UV-cured samples of ESO, ESO/DSO (w/w ratio of 1:0.15), ECHM, and ECHM/DSO (w/w ratio of 1:1.18) from TGA.

Dynamic mechanical properties

The tensile and dynamic mechanical properties of the UV-cured samples after 3 hours and 10 days of storage are summarized in Table 2. The crosslink densities (v_e) were calculated from the storage modulus (E') at 50 °C greater than T_g in the rubbery plateau region (Figure 4.6.a and 4.6.b) following equation (1) (Asif et al., 2005; Chen et al., 2010; Rao and Palanisamy, 2008):

$$E' = 3\nu_e RT \quad (1)$$

where R is the gas constant and T is the absolute temperature. The molecular weight between chain lengths (M_c) was estimated following equation (2):

$$M_c = \frac{d}{\nu_e} \quad (2)$$

where d is the specific gravity of the polymer.

In Table 4.2, the ESO/DSO films showed lower tensile strength than the ECHM/DSO films at both 3 hours and 10 days after UV curing. The apparently low mechanical strengths of the ESO/DSO films were also affected by their low T_g, which were below room temperature, whereas the tensile tests were performed at room temperature, during the samples' rubbery states (Luo et al., 2011). The Tan δ peaks of the ECHM/DSO films at 10 days became narrower compared with those at 3 hours (Figure 4.5 a and 4.5 b). This behavior could be attributed to the post-polymerization of the ECHM/DSO films because the narrower width of Tan δ peaks represented the increase in the homogeneity of polymer networks (Asif et al., 2005; Rao and Palanisamy, 2008); however, the degrees of homogeneity of the ESO/DSO polymer network did not change between 3 hours and 10 days, as indicated by the Tan δ peaks' unchanged widths (Figure 4.5 a and 4.5 b). These results were in accordance with the FTIR analysis as discussed in the previous section, so the change to the more uniform polymer network of the ECHM/DSO films during post-curing could be a convincing reason for increases in their tensile strengths (Table 4.2). Overall, less DSO led to higher crosslink densities for both ESO/DSO and ECHM/DSO films (Table 4.2), which also could be concluded from the width and height of the Tan δ peaks in Figure 5 a and Figure 5 b. Broader Tan δ peak width and lower Tan δ peak height indicated larger crosslink density (Khot et al., 2001).

E' of the ESO/DSO and the ECHM/DSO films was estimated from DMA measurements at 3 hours and 10 days after curing respectively (Figure 4.6 a and 4.6 b). *E'* at the glass transition region of both ESO/DSO and ECHM/ DSO films at 3 hours decreased as DSO contents increased (Figure 4.6 a). In addition, obviously lower *E'* was obtained at both glass transition and

rubbery plateau regions for the films after 10 days of storage with more DSO additions (Figure 4.6 b). The reductions of *E'* and T_g with DSO additions indicated the plasticizing effects of DSO. The increase in *E'* at the rubbery plateau of the ESO/DSO (w/w ratios of 1:0.15 and 1:0.2) and the ECHM/DSO (w/w ratios of 1:1.18 and 1:1.43) at 3 hours after curing (Figure 4.6 a) were caused by heat curing of residual materials during DMA heating (Luo et al., 2011). No significant increases in *E'* of the ESO/DSO (w/w ratios of 1:0.1) and the ECHM/DSO (w/w ratios of 1:1) at 3 hours in their rubbery regions could be explained by a higher degree of polymerization during UV curing due to larger numbers of the epoxy sites under UV irradiation. The larger crosslink densities could effectively disturb polymer chain mobility and curing during DMA heating. *E'* at the rubbery plateau regions of the ESO/DSO and ECHM/DSO films at 10 days after UV curing was higher than at the rubbery region of the samples after 3 hours (Figure 4.6 b). The higher E' in the rubbery region results in the increase of crosslink densities and reductions of molecular weight between chain lengths (Table 4.2).

Table 4.2: Summary of crosslink density, tensile strength, molecular weight between chain length, and elongation of various weight ratios of ESO/DSO and ECHM/DSO at 3hours and 10 days after UV curing.

Monomer/ratio	Cross link density (mol m^{-3})		Tensile strength (MPa)		Molecular weight between chain length (g mol^{-1})		Elongation (%)	
	3hours	10days	3hours	10days	3hours	10days	3hours	10days
ESO:DSO(1:0.1)	1628.3	3376.9	3.9	4.0	655.2	306.7	11.2	11.5
ESO:DSO(1:0.15)	1145.6	1965.9	3.5	3.3	935.5	530.7	11.1	10.4
ESO:DSO(1:0.2)	1181.3	1598.5	3.0	2.7	884.2	658.6	10.4	11.6
ECHM:DSO(1:1)	459.9	584.7	26.8	34.5	2459.6	1833.0	13.4	3.7
ECHM:DSO(1:1.18)	339.1	425.3	19.7	29.5	3306.9	2512.4	21.1	10.3
ECHM:DSO(1:1.43)	332.3	372.1	11.6	15.7	3428.3	2878.1	42.2	44.1

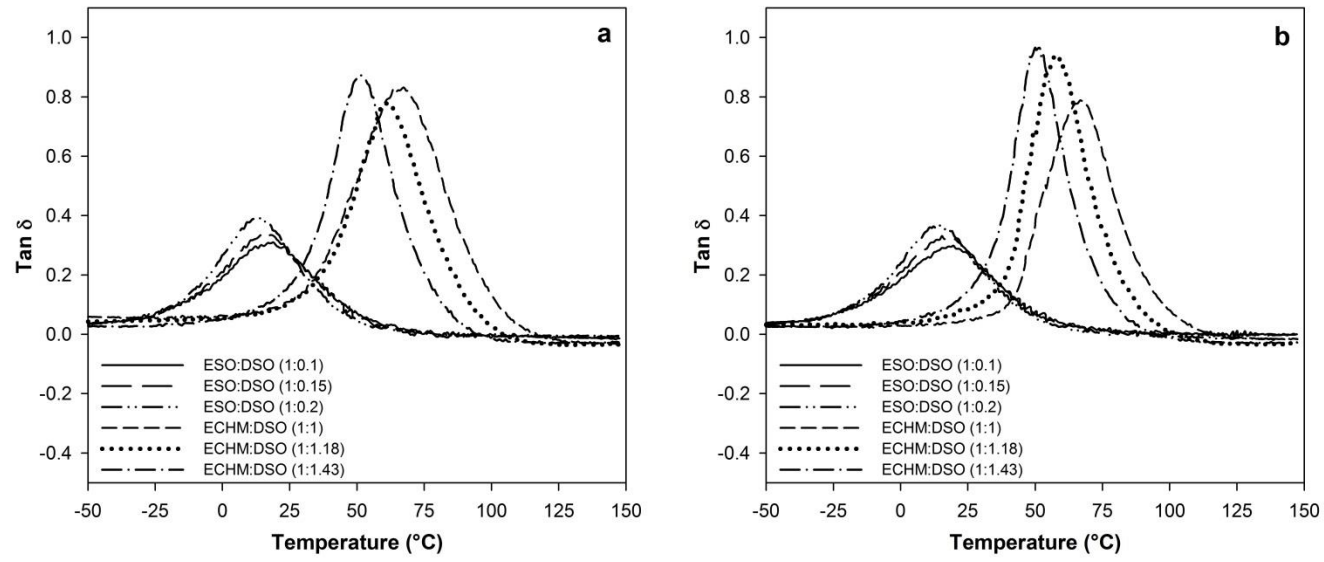

Figure 4.5: Loss factors of ESO/DSO and ECHM/DSO samples at 3hours (a) and 10days (b) after UV curing.

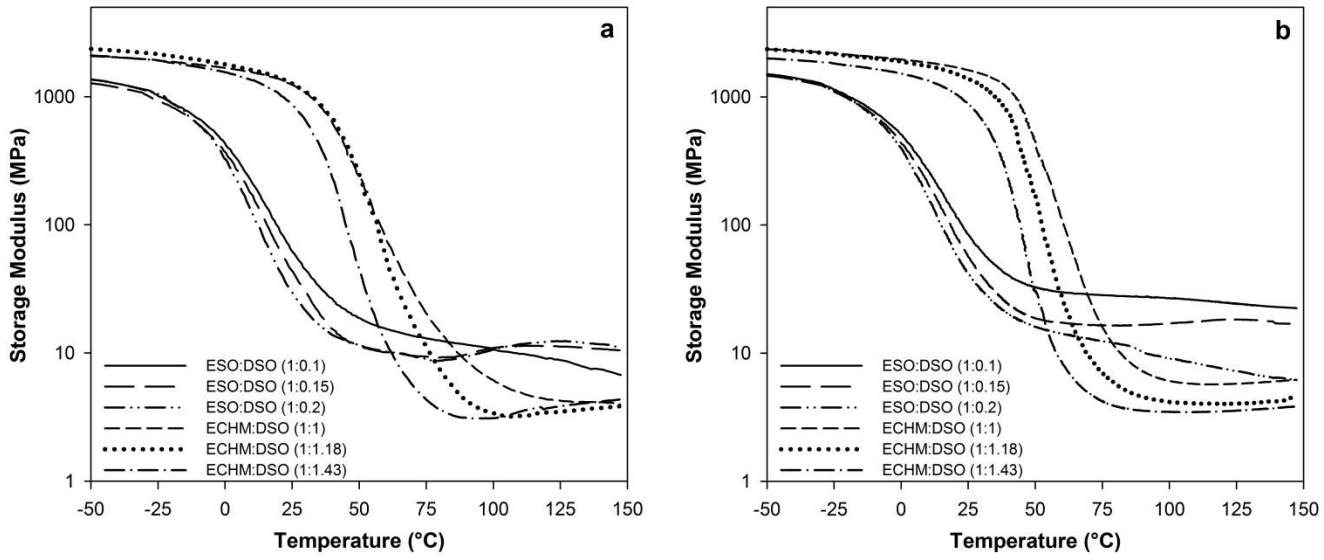

Figure 4.6: Storage modulus of ESO/DSO and ECHM/DSO samples at 3hours (a) and 10days (b) after UV curing.

Tensile properties in shelf life tests

The UV-cured ESO films at weight ratios of ESO:DSO (1:0.1, 1:0.15, and 1:0.2) showed a decrease in tensile strength as DSO contents increased (Figure 4.7). The tensile strengths of all samples increased by approximately 15 to 20 % as storage time approached 1 month. The tensile strengths of the films (w/w ratios of 1:0.1 and 1:0.15) were slightly reduced at 2 months, but the strength of the film (w/w ratio of 1:0.2) remained similar. Elongation at break of the ESO-based films was not affected by DSO additions or storage times. The tensile strength of the ECHM films of all ECHM/DSO ratios was much higher than that of ESO films and decreased significantly as DSO increased. The mechanical strengths of the films were increased by 80 to 140 % during the first month (Figure 4.8). Tensile strength decreased during the 2-month storage time. Elongations at break of the ECHM based films increased significantly as the DSO contents increased, but decreased as storage time increased in the second month.

Overall, both the ESO- and the ECHM-based films reached maximal tensile strength by one month of storage after completion of UV curing, and the ECHM/DSO films showed much higher tensile strength compared with the ESO/DSO films at all storage times. The excellent mechanical strength of the ECHM-based films could be explained by the rigid structure of ECHM itself and the higher reactivity of the external oxiranes (Decker et al., 2001). In addition, increased elongation at break of the ECHM-based films with larger amounts of DSO added was clearly related to the decrement in T_g of the films. A similar result was also reported by Lützen (Luetzen et al., 2013). During our experiments, we found that pure ECHM film could not be peeled from the glass substrate after UV curing due to its highly brittle characteristic. DSO was an effective plasticizer of ECHM to increase the flexibility of the UV-cured ECHM polymer for flexible coating applications.

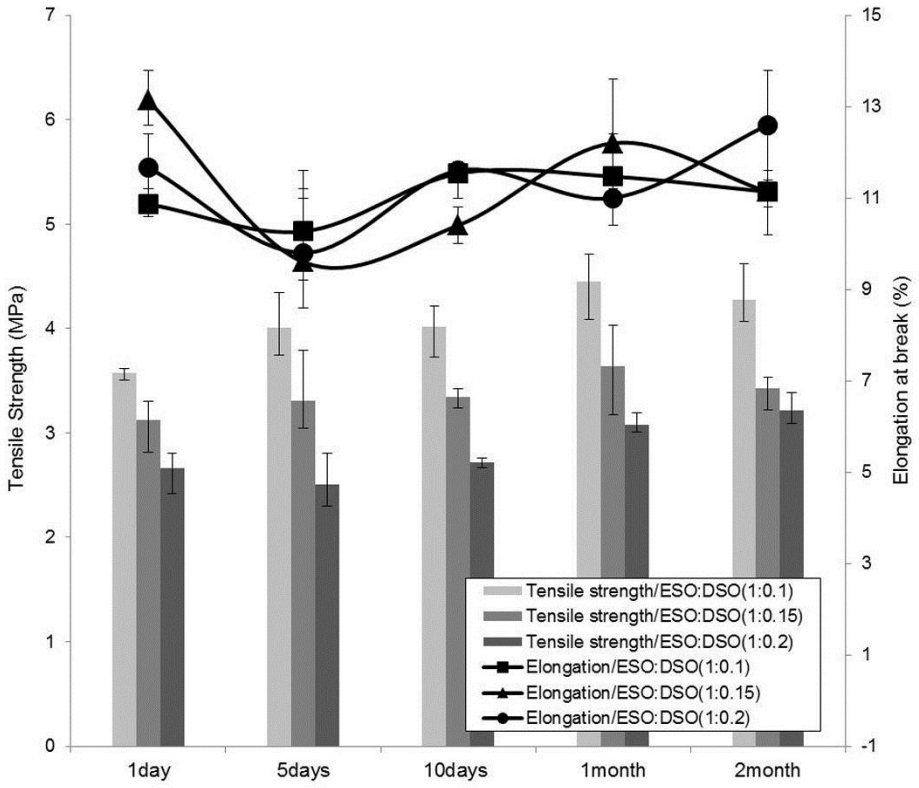

Figure 4.7: Tensile strength and elongation at break of ESO/DSO (w/w ratios of 1:0.1, 1:0.15, and 1:0.2).

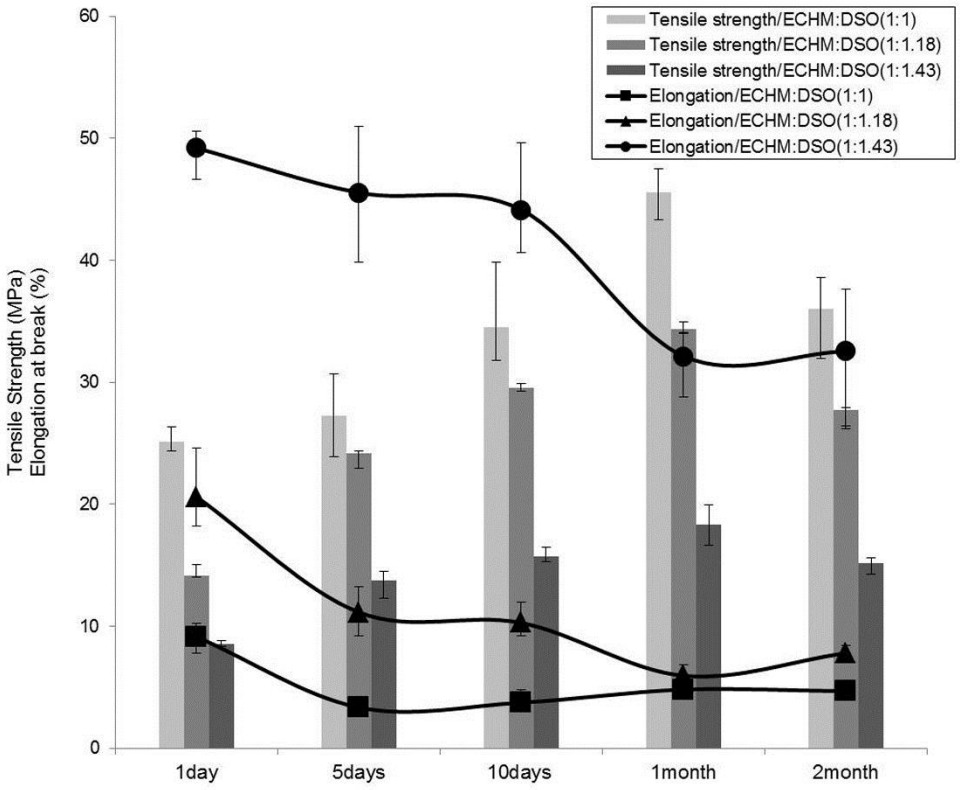

Figure 4.8: Tensile strength and elongation at break of ECHM/DSO (w/w ratios of 1:1, 1:1.18, and 1:1.43).

Optical transmittance

The optical transmittances of the ESO/DSO (w/w ratios of 1:0.15) and the ECHM/DSO (w/w ratios of 1:1.18) were around 90% in the visible light range, their transparency was similar to micro cover glass and PET film (Figure 4.9). In addition, 80% light transmittance of polypropylene and 60% light transmittance of polyethylene in visible ranges were confirmed from our previous research (Ahn et al., 2011a), making the transparencies of the ESO/DSO and the ECHM/DSO UV-cured films comparable to glass and commercial plastics. Accordingly, the bio-based polymers could be useful in transparent coating applications.

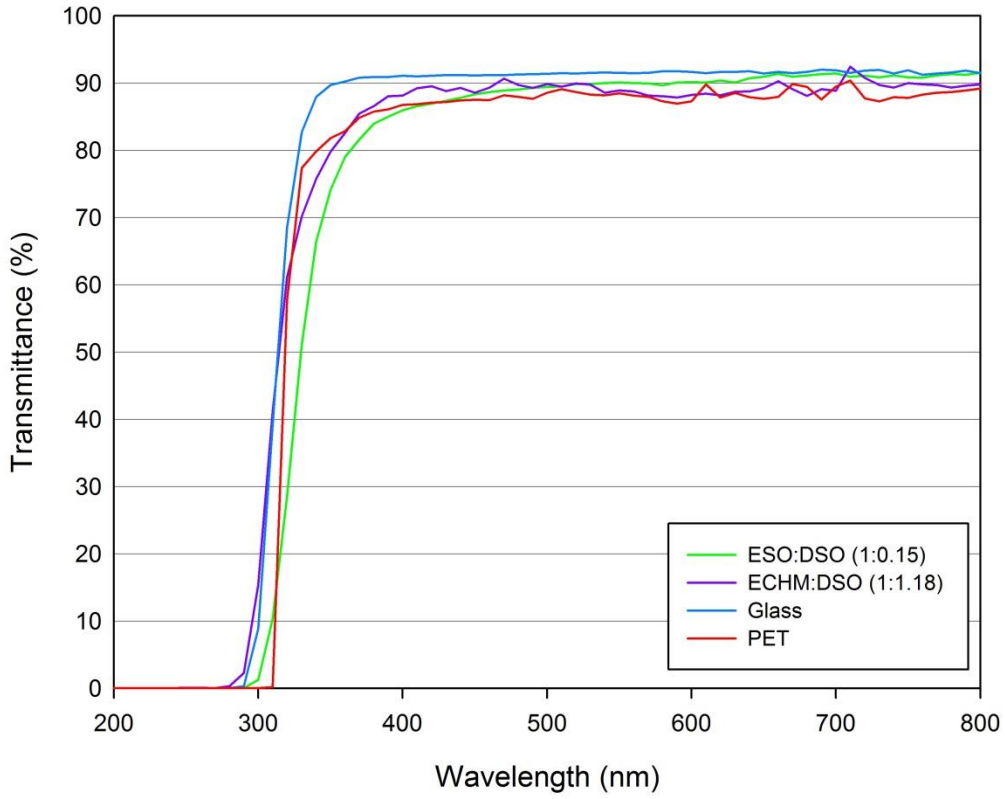

Figure 4.9: Optical transmittances of UV-cued films, micro cover glass, and PET film.

Water uptake properties

The increases of the weights of the ESO/DSO (w/w ratios of of 1:0.2) and the ECHM/DSO (w/w ratios of 1:1.43) were 0.66 ± 0.06% and 2.83 ± 0.2%, respectively, in the water uptake test during 24 hours. Both ESO/DSO and ECHM/DSO polymers exhibited good water resistance. Additionally, the lower water absorption of ESO/DSO could be related to its higher crosslink density.

Chapter 5 - Conclusions

FTIR data indicated that DSO was successfully copolymerized with ESO and ECHM, respectively, to produce bio-based coating materials through UV-initiated cationic ring-opening polymerization. Photopolymerization produced ether cross-linkage polymeric networks in both ESO/DSO and ECHM/DSO copolymers. Tensile strengths of ECHM/DSO films were higher than ESO/DSO films, and glass transition temperatures of ECHM/DSO films were also higher than ESO/DSO films. Tensile strengths, storage modulus, and crosslink densities of UV-cured films were reduced as increases in DSO contents, whereas elongations at breaks were improved. Furthermore, glass transition temperature of UV-cured films decreased as DSO contents increased in the polymers. Therefore, DSO was found to be an effective plasticizer for both ESO and ECHM systems.

The ECHM/DSO (w/w ratio of 1:1.43) film showed excellent flexibility during the shelf life tested in this study. ESO/DSO (w/w ratio of 1:1) and ECHM/DSO (w/w ratio of 1:1.18) films exhibited the highest tensile strengths. Mechanical properties of the soybean-based UV-cured films remained stable during the 2-month shelf life. Post-polymerization effects were confirmed by spectral, thermal, mechanical, and dynamic mechanical analyses. The transparencies of soybean-based UV-cured films were similar to that of micro cover glass and PET films. In addition, both ESO/DSO and ECHM/DSO UV-cured films showed good water resistances.

The soybean oil-based UV-curable films showed great potential for transparent flexible coating applications, and DSO exhibited excellent abilities as a plasticizer for both bio-based epoxy resin and petrochemical-based epoxy resin.

References

Adeodato Vieira, M. G., da Silva, M. A., dos Santos, L. O., and Beppu, M. M. (2011). Natural-based plasticizers and biopolymer films: A review. *European Polymer Journal,* 47: 254-263. doi:10.1016/j.eurpolymj.2010.12.011

Afrifah, K. A., and Matuana, L. M. (2010). Impact modification of polylactide with a biodegradable ethylene/acrylate copolymer. *Macromolecular Materials and Engineering,* 295: 802-811. doi:10.1002/mame.201000107

Ahn, B. K., Kraft, S., Wang, D., and Sun, X. S. (2011a). Thermally stable, transparent, pressure-sensitive adhesives from epoxidized and dihydroxyl soybean oil. *Biomacromolecules,* 12: 1839-1843. doi:10.1021/bm200188u

Ahn, B. K., Sung, J., Kim, N., Kraft, S., and Sun, X. S. (2013). UV-curable pressure-sensitive adhesives derived from functionalized soybean oils and rosin ester. *Polymer International,* 62: 1293-1301. doi:10.1002/pi.4420

Ahn, B. K., Sung, J., Rahmani, N., Wang, G., Kim, N., Lease, K., and Sun, X. S. (2013). UV-curable, high-shear pressure-sensitive adhesives derived from acrylated epoxidized soybean oil. *Journal of Adhesion,* 89: 323-338. doi:10.1080/00218464.2013.749102

Ahn, B. K., Kraft, S., and Sun, X. S. (2011b). Chemical pathways of epoxidized and hydroxylated fatty acid methyl esters and triglycerides with phosphoric acid. *Journal of Materials Chemistry,* 21: 9498-9505. doi:10.1039/c1jm10921a

Asif, A., Shi, W. F., Shen, X. F., and Nie, K. M. (2005). Physical and thermal properties of UV curable waterborne polyurethane dispersions incorporating hyperbranched aliphatic polyester of varying generation number. *Polymer,* 46: 11066-11078. doi:10.1016/j.polymer.2005.09.046

Aulin, C., Salazar-Alvarez, G., and Lindstrom, T. (2012). High strength, flexible and transparent nanofibrillated cellulose-nanoclay biohybrid films with tunable oxygen and water vapor permeability. *Nanoscale,* 4: 6622-6628. doi:10.1039/c2nr31726e

Avenabustillos, R. J., and Krochta, J. M. (1993). Water-vapor permeability of caseinate-based edible films as affected by ph, calcium cross-linking and lipid-content. *Journal of Food Science,* 58: 904-907. doi:10.1111/j.1365-2621.1993.tb09388.x

Baltacioglu, H., and Balkose, D. (1999). Effect of zinc stearate and/or epoxidized soybean oil on celation and thermal stability of PVC-DOP plastigels. *Journal of Applied Polymer Science,* 74: 2488-2498. doi:10.1002/(SICI)1097-4628(19991205)74:10<2488::AID-APP18>3.0.CO;2-B

Basturk, E., Inan, T., and Gungor, A. (2013). Flame retardant UV-curable acrylated epoxidized soybean oil based organic-inorganic hybrid coating. *Progress in Organic Coatings,* 76: 985-992. doi:10.1016/j.porgcoat.2012.10.007

Bueno-Ferrer, C., Garrigos, M. C., and Jimenez, A. (2010). Characterization and thermal stability of poly(vinyl chloride) plasticized with epoxidized soybean oil for food packaging. *Polymer Degradation and Stability,* 95: 2207-2212. doi:10.1016/j.polymdegradstab.2010.01.027

Campanella, A., La Scala, J. J., and Wool, R. P. (2009). The use of acrylated fatty acid methyl esters as styrene replacements in triglyceride-based thermosetting polymers. *Polymer Engineering and Science*, 49: 2384-2392. doi:10.1002/pen.21486

Chan, M. A., and Krochta, J. M. (2001). Grease and oxygen barrier properties of whey-protein-isolate coated paperboard, *Tappi J,* 84: 57.

Chen, Z., Chisholm, B. J., Patani, R., Wu, J. F., Fernando, S., Jogodzinski, K., and Webster, D. C. (2010). Soy-based UV-curable thiol-ene coatings. *Journal of Coatings Technology and Research,* 7: 603-613. doi:10.1007/s11998-010-9241-x

Chiang, T. H., and Hsieh, T. E. (2006). A study of monomer's effect on adhesion strength of UV-curable resins. *International Journal of Adhesion and Adhesives,* 26: 520-531. doi:10.1016/j.ijadhadh.2005.07.004

Cho, J. D., and Hong, J. W. (2004). UV-initiated free radical and cationic photopolymerizations of acrylate/ep oxide and acrylate/vinyl ether hybrid systems with and without photosensitizer. *Journal of Applied Polymer Science,* 93: 1473-1483. doi:10.1002/app.20597

Cho, J. D., Kim, H. K., Kim, Y. S., and Hong, J. W. (2003). Dual curing of cationic UV-curable clear and pigmented coating systems photosensitized by thioxanthone and anthracene. *Polymer Testing,* 22: 633-645. doi:10.1016/S0142-9418(02)00169-1

Choi, J. S., and Park, W. H. (2004). Effect of biodegradable plasticizers on thermal and mechanical properties of poly (3-hydroxybutyrate). *Polymer Testing,* 23: 455-460. doi:10.1016/j.polymertesting.2003.09.005

Crivello, J. V., and Linzer, V. (1998). Study of the structure-reactivity relationships in the photoinitiated cationic polymerization of epoxide monomers. *Polimery,* 43: 661-672.

Crivello, J. V., and Liu, S. S. (2000). Photoinitiated cationic polymerization of epoxy alcohol monomers. *Journal of Polymer Science Part A-Polymer Chemistry,* 38: 389-401. doi:10.1002/(SICI)1099-0518(20000201)38:3<389::AID-POLA1>3.0.CO;2-G

Crivello, J. V., and Narayan, R. (1992). Epoxidized triglycerides as renewable monomers in photoinitiated cationic polymerization. *Chemistry of Materials,* 4: 692-699. doi:10.1021/cm00021a036

Crivello, J. V., Conlon, D. A., Olson, D. R., and Webb, K. K. (1986). The effects of polyols as chain-transfer agents and flexibilizers in photoinitiated cationic polymerization. *Journal of Radiation Curing,* 13: 2.

Czub, P. (2006). Application of modified natural oils as reactive diluents for epoxy resins. *Macromolecular Symposia,* 242: 60-64. doi:10.1002/masy.200651010

Decker, C., Viet, T. T. N., and Thi, H. P. (2001). Photoinitiated cationic polymerization of epoxides. *Polymer International,* 50: 986-997. doi:10.1002/pi.730

Del Rio, E., Galia, M., Cadiz, V., Lligadas, G., and Ronda, J. C. (2010). Polymerization of epoxidized vegetable oil derivatives: Ionic-coordinative polymerization of methylepoxyoleate. *Journal of Polymer Science Part A-Polymer Chemistry,* 48: 4995-5008. doi:10.1002/pola.24297

Dillman, B., and Jessop, J. L. P. (2013). Chain transfer agents in cationic photopolymerization of a bis-cycloaliphatic epoxide monomer: Kinetic and physical property effects. *Journal of Polymer Science Part A-Polymer Chemistry,* 51: 2058-2067. doi:10.1002/pola.26595

Drumright, R., Gruber, P., and Henton, D. (2000). Polylactic acid technology. *Advanced Materials,* 12: 1841-1846. doi:10.1002/1521-4095(200012)12:23<1841::AID-ADMA1841>3.0.CO;2-E

Espana, J. M., Sanchez-Nacher, L., Boronat, T., Fombuena, V., and Balart, R. (2012). Properties of biobased epoxy resins from epoxidized soybean oil (ESBO) cured with maleic anhydride

(MA). *Journal of the American Oil Chemists Society,* 89: 2067-2075. doi:10.1007/s11746-012-2102-2

Fouassier, J. P., and Rabek, J. F. (1993). *Radiation curing in polymer science and technology*. London: Elsevier Applied Science.

Frados, J. (1976). *Plastics engineering handbook of the society of the plastics industry, inc.* New York: Van Nostrand Reinhold.

Gallstedt, M., and Hedenqvist, M. S. (2004). Packaging-related properties of alkyd-coated, wax-coated, and buffered chitosan and whey protein films. *Journal of Applied Polymer Science,* 91: 60-67. doi:10.1002/app.13218

Garcia, M. A., Martino, M. N., and Zaritzky, N. E. (2000). Lipid addition to improve barrier properties of edible starch-based films and coatings. *Journal of Food Science,* 65: 941-947. doi:10.1111/j.1365-2621.2000.tb09397.x

Golaz, B., Michaud, V., Leterrier, Y., and Manson, J. -. E. (2012). UV intensity, temperature and dark-curing effects in cationic photo-polymerization of a cycloaliphatic epoxy resin. *Polymer,* 53: 2038-2048. doi:10.1016/j.polymer.2012.03.025

Guner, F. S., Yagci, Y., and Erciyes, A. T. (2006). Polymers from triglyceride oils. *Progress in Polymer Science,* 31: 633-670. doi:10.1016/j.progpolymsci.2006.07.001

Gunstone, F. D. (2004). *The chemistry of oils and fats: Sources, composition, properties and uses.* 9600 Garsington Rd., Oxford OX4 2DQ, UK; Blackwell Publishing Ltd. Tel. +44 (0)1865 776868. wwwblackwellpublishing.com. Price GBP 95.00:

Guo, A., Cho, Y. J., and Petrovic, Z. S. (2000). Structure and properties of halogenated and nonhalogenated soy-based polyols. *Journal of Polymer Science Part A-Polymer Chemistry,* 38: 3900-3910. doi:10.1002/1099-0518(20001101)38:21<3900::AID-POLA70>3.0.CO;2-E

Gupta, A. P., Ahmad, S., and Dev, A. (2011). Modification of novel bio-based resin-epoxidized soybean oil by conventional epoxy resin. *Polymer Engineering and Science,* 51: 1087-1091. doi:10.1002/pen.21791

Holland, J. M., Lewis, M., and Nelson, A. (2003a). Desymmetrization of a centrosymmetric diepoxide: Efficient synthesis of a key intermediate in a total synthesis of hemibrevetoxin B. *Journal of Organic Chemistry,* 68: 747-753. doi:10.1021/jo026456b

Holland, J. M., Lewis, M., and Nelson, A. (2003b). Desymmetrization of a centrosymmetric diepoxide: Efficient synthesis of a key intermediate in a total synthesis of hemibrevetoxin B. *Journal of Organic Chemistry,* 68: 747-753. doi:10.1021/jo026456b

Inan, T. Y., Ekinci, E., Yildiz, E., Kuyulu, A., and Gungor, A. (2001). Preparation and characterization of novel UV-curable urethane methacrylate difunctional monomers and their structure-property relationships, 1. *Macromolecular Chemistry and Physics*, 202: 532-540.

Kester, J. J., and Fennema, O. R. (1986). Edible films and coatings - a review. *Food Technology,* 40: 47-59.

Khot, S. N., Lascala, J. J., Can, E., Morye, S. S., Williams, G. I., Palmese, G. R., Kusefoglu, S. H., and Wool, R. P. (2001). Development and application of triglyceride-based polymers and composites. *Journal of Applied Polymer Science,* 82: 703-723. doi:10.1002/app.1897

Khwaldia, K., Arab-Tehrany, E., and Desobry, S. (2010). Biopolymer coatings on paper packaging materials. *Comprehensive Reviews in Food Science and Food Safety,* 9: 82-91. doi:10.1111/j.1541-4337.2009.00095.x

Kundu, P. P., and Larock, R. C. (2005). Novel conjugated linseed oil-styrene-divinylbenzene copolymers prepared by thermal polymerization. 1. effect of monomer concentration on the structure and properties. *Biomacromolecules,* 6: 797-806. doi:10.1021/bm049429z

Lee, S., Kang, I., Doh, G., Yoon, H., Park, B., and Wu, Q. (2008). Thermal and mechanical properties of wood flour/talc-filled polylactic acid composites: Effect of filler content and coupling treatment. *Journal of Thermoplastic Composite Materials,* 21: 209-223. doi:10.1177/0892705708089473

Liu, Z. S., Erhan, S. Z., and Calve, P. D. (2004). Solid freeform fabrication of epoxidized soybean oil/epoxy composites with di-, tri-, and polyethylene amine curing agents. *Journal of Applied Polymer Science,* 93: 356-363. doi:10.1002/app.20412

Liu, Z., Erhan, S., and Xu, J. (2005). Preparation, characterization and mechanical properties of epoxidized soybean oil/clay nanocomposites. *Polymer,* 46: 10119-10127. doi:10.1016/j.polymer.2005.08.065

Lligadas, G., Ronda, J. C., Galia, M., and Cadiz, V. (2006). Bionanocomposites from renewable resources: Epoxidized linseed oil-polyhedral oligomeric silsesquioxanes hybrid materials. *Biomacromolecules,* 7: 3521-3526. doi:10.1021/bm060703u

Lu, J., Hong, C. K., and Wool, R. P. (2004). Bio-based nanocomposites from functionalized plant oils and layered silicate. *Journal of Polymer Science Part B-Polymer Physics,* 42: 1441-1450. doi:10.1002/polb.20027

Luetzen, H., Bitomsky, P., Rezwan, K., and Hartwig, A. (2013). Partially crystalline polyols lead to morphology changes and improved mechanical properties of cationically polymerized epoxy resins. *European Polymer Journal,* 49: 167-176. doi:10.1016/j.eurpolymj.2012.10.015

Luo, Q., Liu, M., Xu, Y., Ionescu, M., and Petrovic, Z. S. (2011). Thermosetting allyl resins derived from soybean oil. *Macromolecules,* 44: 7149-7157. doi:10.1021/ma201366e

Martino, V. P., Jiménez, A., and Ruseckaite, R. A. (2009). Processing and characterization of poly(lactic acid) films plasticized with commercial adipates. *Journal of Applied Polymer Science,* 112: 2010-2018. doi:10.1002/app.29784

Meier, M. A. R., Metzger, J. O., and Schubert, U. S. (2007). Plant oil renewable resources as green alternatives in polymer science. *Chemical Society Reviews,* 36: 1788-1802. doi:10.1039/b703294c

Miao, S., Zhang, S., Su, Z., and Wang, P. (2013). Synthesis of bio-based polyurethanes from epoxidized soybean oil and isopropanolamine. *Journal of Applied Polymer Science,* 127: 1929-1936. doi:10.1002/app.37564

Mihail, I., and Petrovic, Z. S. (2011). Polymerization of soybean oil with superacids. *Soybean: Applications and Technology*, : 365. doi:10.5772/10547

Mol, J. (2002). Application of olefin metathesis in oleochemistry: An example of green chemistry. *Green Chemistry,* 4: 5-13. doi:10.1039/b109896a

Murtaza, G. (2012). Ethylcellulose microparticles: A review. *Acta Poloniae Pharmaceutica - Drug Research,* 69: 11-22.

Otaigbe, J. U., and Adams, D. O. (1997). Bioabsorbable soy protein plastic composites: Effect of polyphosphate fillers on water absorption and mechanical properties. *Journal of Environmental Polymer Degradation,* 5: 199-208.

Ozturk, C., and Kusefoglu, S. H. (2011). Polymerization of epoxidized soybean oil with maleinized polybutadiene. *Journal of Applied Polymer Science,* 120: 116-123. doi:10.1002/app.33094

Parreira, T. F., Ferreira, M. M. C., Sales, H. J. S., and de Almeida, W. B. (2002). Quantitative determination of epoxidized soybean oil using near-infrared spectroscopy and multivariate calibration. *Applied Spectroscopy,* 56: 1607-1614. doi:10.1366/000370202321115887

Petrovic, Z. S., Guo, A., and Zhang, W. (2000). Structure and properties of polyurethanes based on halogenated and nonhalogenated soy-polyols. *Journal of Polymer Science Part A-Polymer Chemistry,* 38: 4062-4069. doi:10.1002/1099-0518(20001115)38:22<4062::AID-POLA60>3.0.CO;2-L

Petrovic, Z. (2008). Polyurethanes from vegetable oils. *Polymer Reviews,* 48: 109-155. doi:10.1080/15583720701834224

Pilla, S., Gong, S., O'Neill, E., Rowell, R. M., and Krzysik, A. M. (2008). Polylactide-pine wood flour composites. *Polymer Engineering & Science,* 48: 578-587. doi:10.1002/pen.20971

Rangasai, M. C., Bhosale, S. H., Singh, V. V., and Ghosh, S. B. (2014). Incorporation of epoxidized soybean oil as co-matrix in epoxy resin toward developing plastisol/particulate toughened glass fiber composites. *Journal of Applied Polymer Science,* 131: 40586. doi:10.1002/app.40586

Rao, B. S., and Palanisamy, A. (2008). Synthesis, photo curing and viscoelastic properties of triacrylate compositions based on ricinoleic acid amide derived from castor oil. *Progress in Organic Coatings,* 63: 416-423. doi:10.1016/j.porgcoat.2008.07.001

Rengasamy, S., and Mannari, V. (2013). Development of soy-based UV-curable acrylate oligomers and study of their film properties. *Progress in Organic Coatings,* 76: 78-85. doi:10.1016/j.porgcoat.2012.08.012

Rhee, G. S., Kim, S. H., Kim, S. S., Sohn, K. H., Kwack, S. J., Kim, B. H., and Park, K. L. (2002). Comparison of embryotoxicity of ESBO and phthalate esters using an in vitro battery system. *Toxicology in Vitro,* 16: 443-448.

Rhim, J. W., Lee, J. H., and Hong, S. I. (2006). Water resistance and mechanical properties of biopolymer (alginate and soy protein) coated paperboards. *Lwt-Food Science and Technology,* 39: 806-813. doi:10.1016/j.lwt.2005.05.008

Rhim, J. W., Mohanty, K. A., Singh, S. P., and Ng, P. K. W. (2006). Preparation and properties of biodegradable multilayer films based on soy protein isolate and poly(lactide). *Industrial & Engineering Chemistry Research,* 45: 3059-3066. doi:10.1021/ie051207+

Robertson, M. L., Chang, K., Gramlich, W. M., and Hillmyer, M. A. (2010). Toughening of polylactide with polymerized soybean oil. *Macromolecules,* 43: 1807-1814. doi:10.1021/ma9022795

Rosen, S. L. (1993). *Fundamental principles of polymeric materials*. New York [etc.]: John Wiley and Sons.

Schreck, K. M., and Hillmyer, M. A. (2007). Block copolymers and melt blends of polylactide with nodax™ microbial polyesters: Preparation and mechanical properties. *Journal of Biotechnology,* 132: 287-295. doi:http://dx.doi.org/10.1016/j.jbiotec.2007.03.017

Sejidov, F. T., Mansoori, Y., and Goodarzi, N. (2005). Esterification reaction using solid heterogeneous acid catalysts under solvent-less condition. *Journal of Molecular Catalysis A-Chemical,* 240: 186-190. doi:10.1016/j.molcata.2005.06.048

Seydibeyoglu, M. O., Misra, M., Mohanty, A., Blaker, J. J., Lee, K., Bismarck, A., and Kazemizadeh, M. (2013). Green polyurethane nanocomposites from soy polyol and

bacterial cellulose. *Journal of Materials Science,* 48: 2167-2175. doi:10.1007/s10853-012-6992-z

Shibata, M., Teramoto, N., Someya, Y., and Suzuki, S. (2009). Bio-based nanocomposites composed of photo-cured epoxidized soybean oil and supramolecular hydroxystearic acid nanofibers. *Journal of Polymer Science Part B-Polymer Physics,* 47: 669-673. doi:10.1002/polb.21671

Sipani, V., and Scranton, A. B. (2003). Dark-cure studies of cationic photopolymerizations of epoxides: Characterization of the active center lifetime and kinetic rate constants. *Journal of Polymer Science Part A-Polymer Chemistry,* 41: 2064-2072. doi:10.1002/pola.10750

Siracusa, V., Rocculi, P., Romani, S., and Dalla Rosa, M. (2008). Biodegradable polymers for food packaging: A review. *Trends in Food Science & Technology,* 19: 634-643. doi:10.1016/j.tifs.2008.07.003

Sogol, K., and Ismaeil, H. (2011). Mechanical influence of static versus dynamic loadings on parametrical analysis of plasticized ethyl cellulose films. *International Journal of Pharmaceutics,* 408: 1-8. doi:http://dx.doi.org/10.1016/j.ijpharm.2010.11.031

Starnes, W. H. (2002). Structural and mechanistic aspects of the thermal degradation of poly(vinyl chloride). *Progress in Polymer Science,* 27: 2133-2170. doi:10.1016/S0079-6700(02)00063-1

Svagan, A. J., Akesson, A., Cardenas, M., Bulut, S., Knudsen, J. C., Risbo, J., and Plackett, D. (2012). Transparent films based on PLA and montmorillonite with tunable oxygen barrier properties. *Biomacromolecules,* 13: 397-405. doi:10.1021/bm201438m

Tharanathan, R. N. (2003). Biodegradable films and composite coatings: Past, present and future. *Trends in Food Science & Technology,* 14: 71-78. doi:10.1016/S0924-2244(02)00280-7

Thulasiraman, V., Rakesh, S., and Sarojadevi, M. (2009). Synthesis and characterization of chlorinated soy oil based epoxy resin/glass fiber composites. *Polymer Composites,* 30: 49-58. doi:10.1002/pc.20532

Tokiwa, Y., Calabia, B., Ugwu, C., and Aiba, S. (2009). Biodegradability of plastics. *International Journal of Molecular Sciences,* 10: 3722-3742. doi:10.3390/ijms10093722

Uyama, H., Kuwabara, M., Tsujimoto, T., Nakano, M., Usuki, A., and Kobayashi, S. (2003). Green nanocomposites from renewable resources: Plant oil-clay hybrid materials. *Chemistry of Materials,* 15: 2492-2494. doi:10.1021/cm0340227

Veronese, V. B., Menger, R. K., Forte, M. M. d. C., and Petzhold, C. L. (2011). Rigid polyurethane foam based on modified vegetable oil. *Journal of Applied Polymer Science,* 120: 530-537. doi:10.1002/app.33185

Vijayarajan, S., Selke, S. E. M., and Matuana, L. M. (2014). Continuous blending approach in the manufacture of epoxidized SoybeanPlasticized poly(lactic acid) sheets and films. *Macromolecular Materials and Engineering,* 299: 622-630. doi:10.1002/mame.201300226

Voytekunas, V. Y., Ng, F. L., and Abadie, M. J. M. (2008). Kinetics study of the UV-initiated cationic polymerization of cycloaliphatic diepoxide resins. *European Polymer Journal,* 44: 3640-3649. doi:10.1016/j.eurpolymj.2008.08.043

Williams, C. K., and Hillmyer, M. A. (2008). Polymers from renewable resources: A perspective for a special issue of polymer reviews. *Polymer Reviews,* 48: 1-10. doi:10.1080/15583720701834133

Wool, R. P., and Sun, X. S. (2005). *Bio-based polymers and composites* (1st ed.). Amsterdam, Boston: Elsevier Academic Press.

Wu, J. F., Fernando, S., Jagodzinski, K., Weerasinghe, D., and Chen, Z. (2011). Effect of hyperbranched acrylates on UV-curable soy-based biorenewable coatings. *Polymer International,* 60: 571-577. doi:10.1002/pi.2980

Xia, Y., and Larock, R. C. (2010). Vegetable oil-based polymeric materials: Synthesis, properties, and applications. *Green Chemistry,* 12: 1893-1909. doi:10.1039/c0gc00264j

Yang, D., Peng, X., Zhong, L., Cao, X., Chen, W., Zhang, X., Liu, S., and Sun, R. (2014). "Green" films from renewable resources: Properties of epoxidized soybean oil plasticized ethyl cellulose films. *Carbohydrate Polymers,* 103: 198-206. doi:10.1016/j.carbpol.2013.12.043

Zhang, C., Ding, R., and Kessler, M. R. (2014). Reduction of epoxidized vegetable oils: A novel method to prepare bio-based polyols for polyurethanes. *Macromolecular Rapid Communications,* 35: 1068-1074. doi:10.1002/marc.201400039

Zhang, C., Xia, Y., Chen, R., Huh, S., Johnston, P. A., and Kessler, M. R. (2013). Soy-castor oil based polyols prepared using a solvent-free and catalyst-free method and polyurethanes therefrom. *Green Chemistry,* 15: 1477-1484. doi:10.1039/c3gc40531a